The Impact of Currency Carry Trade Activity on the Transmission of Monetary Policy*

Maximilian Boeck[1], Alina Steshkova[2], and Thomas O. Zörner[3]

[1] Bocconi University
[2] Vienna University of Economics and Business, Research Institute for Capital Markets
[3] Oesterreichische Nationalbank (OeNB)

First Version: March 2023
This Version: August 2024

Abstract

This paper examines how carry trade activity affects the transmission of monetary policy in currency markets. It analyzes a set of developed and emerging market currencies against the U.S. dollar. The U.S. dollar appreciates in response to a conventional monetary policy shock but depreciates to a central bank information shock. A threshold vector autoregressive model is fitted to discriminate between different regimes of speculative carry trade activity. Higher carry trade intensity is associated with larger excess returns and higher crash risk. Across regimes, the differences in exchange rates are mild, while those in interest rates are more pronounced. A currency trading strategy created on the day of central bank announcements, which takes into consideration the joint co-movement of interest rates and stock prices, substantially outperforms the carry trade in terms of the Sharpe ratio and downside risk.

Keywords: Currency markets, Carry Trade Strategy, Monetary Policy, Threshold VAR
JEL Codes: C24, C32, E52, F31, F41

*Alina Steshkova, Research Institute for Capital Markets, Vienna University of Economics and Business, Welthandelsplatz 1, 1020 Vienna. E-mail: alina.steshkova@wu.ac.at. Maximilian Boeck, Bocconi University, Department of Economics, Via Roentgen, 1 Milano, Italy. E-mail: maximilian.boeck@unibocconi.it. Thomas O. Zörner, Monetary Policy Section, Oesterreichische Nationalbank. Otto-Wagner-Platz 3, 1090 Vienna, Austria. E-mail: thomas.zoerner@oenb.at.
We thank Paolo Cavallino, Georg Cejnek, Thomas Dangl, Pia Heckl, Florian Huber, Zhengyang Jiang, Ingrid Kubin, Hanno Lustig, Stefan Pichler, Daria Prem, Otto Randl, Ákos Török, Andrea Vedolin, Clinton Watkins, Josef Zechner, and Irina Zviadadze for helpful suggestions and valuable comments. Frane Gudelj provided excellent research assistance. We gratefully acknowledge helpful comments from the participants of the the 27th International Conference on Macroeconomic Analysis and International Finance (University of Crete), the Annual Congress of the Swiss Society of Economics and Statistics (University Neuchâtel), the 2023 Annual Meeting of the Central Bank Research Association (Columbia University), the 29th Annual Meeting of the German Finance Association (Verein für Socialpolitik), and the Conference of Frankfurt Institute for Risk Management and Regulation (FIRM).

1 Introduction

Foreign exchange (FX) markets are driven not only by economic fundamentals, but also by speculative trading activities. A popular strategy, the currency carry trade, exploits interest rate differentials by borrowing in low interest rate currencies and investing in high interest rate currencies. This strategy systematically generates excess returns and is associated with elevated volatility in FX markets and currency crash risks (Brunnermeier, Nagel and Pedersen, 2008; Burnside, Eichenbaum and Rebelo, 2011; Mueller, Tahbaz-Salehi and Vedolin, 2017; Zviadadze, 2017). As the international financial system is centered around the U.S., its monetary policy actions affect interest rate differentials, which impact the profitability and risk profile of this strategy. However, monetary policy decisions of the Federal Reserve (Fed) convey information about both monetary policy and future economic conditions, potentially impacting exchange rates in different directions.[1] This paper investigates the impact of monetary policy actions on exchange rates and excess returns, by considering their effects during episodes of high carry trade activity.

This paper empirically investigates the relationship between U.S. monetary policy and exchange rates vis-à-vis the U.S. dollar across 15 advanced and emerging economies. We first develop a linear vector autoregressive (VAR) model to assess the impact of monetary policy shocks on exchange rates. Our VAR framework is based on the recent theoretical model of Jiang, Lustig and Krishnamurthy (2021). It links the U.S. dollar exchange rate to the concept of *convenience yields* of U.S. Treasuries – safe and highly liquid assets – thus incorporating the significant global role of the U.S. dollar. For identifying monetary policy shocks, we apply the procedure from Jarociński and Karadi (2020), which distinguishes between monetary and information shocks by analyzing the co-movement between interest rate and stock market surprises. A negative co-movement indicates a conventional *monetary policy* shock, while a positive co-movement is interpreted as an *central bank information* shock.[2] Second, we use a non-linear threshold VAR model to analyze the effects of these shocks on exchange rates, conditional on the intensity of speculative carry trade activity in the respective currency market. We identify different regimes of carry trade activity for a subset of seven currencies based on their distinct risk profiles and assess the impact of both shocks within these regimes. To proxy speculative carry trade activity, we use the *net open interest*, defined as the difference between long and short futures positions of non-commercial traders in the foreign currency, divided by the total open interest of all traders. (Brunnermeier, Nagel and Pedersen, 2008; Fong, 2013).

We expect that an unanticipated monetary tightening leads to an appreciation of the U.S. dollar as U.S. Treasuries become more attractive and to a deterioration of economic conditions. However, a monetary tightening accompanied by an increase in stock prices points in the opposite direction, namely an improvement in the respective sentiments where the U.S. dollar will depreciate. This is mainly due to a substitution effect

[1] Economic theory suggests that in general a tightening of monetary policy leads – ceteris paribus – to an immediate appreciation of the domestic currency. However, the domestic currency may also depreciate to a non-anticipated increase in the interest rate, depending on the nature of the shock originating from the central bank (see, for instance, Dornbusch, 1976; Eichenbaum and Evans, 1995; Faust and Rogers, 2003; Rogers, Scotti and Wright, 2018; Pinchetti and Szczepaniak, 2023).

[2] We follow the bulk of the literature, which denotes this shock as an *central bank information* or *growth* shock. The common interpretation is that a central bank reveals non-public information, thus shaping private sectors' expectations (Melosi, 2017; Nakamura and Steinsson, 2018; Cieslak and Schrimpf, 2019). Recently, this has been challenged by Bauer and Swanson (2023a), pointing to a "Fed response to news" channel, where both the central bank and the market react to incoming economic news in the days and weeks leading up to an announcement. The central bank reacts more strongly to these news than the public had expected. As a result, professional forecasters revise their forecasts, leading to a procyclical correlation with monetary policy surprises.

of safe assets' demand by search-for-yield motives. Hence, we expect that monetary policy and information shocks lead to different exchange rate adjustment dynamics. The question arises how investors react to these shocks when taking carry trade activity into account. By affecting interest rate differentials investors might be forced to unwind their positions to limit losses or settle margin calls. This increases the pressure on the respective exchange rates and the profitability of the currency carry trade, observed through excess returns. Higher speculative trading activity may thus lead to losses and increased crash risk. Given the specific risk profiles of different currencies, we expect to observe varying dynamics for safe-haven and high-yielding currencies across different regimes of speculative carry trade intensity.

We find that both shocks affect exchange rates, but in opposite directions. A contractionary monetary policy shock causes an appreciation of the U.S. dollar, while an information shock associated with higher interest rates results in a depreciation. While the monetary policy shock leads to an increase in global risk aversion, the central bank information shock has a dampening effect on the risk-absorbing capacity of international financial markets. This strongly aligns with the interpretation of the information shock as growth news shock. The magnitude of these reactions varies by currency, due to the currency's risk characteristics and attractiveness for speculative trading. There is also heterogeneity in the responses, as the U.S. dollar depreciates not against all currencies – particularly, safe-haven currencies. In the non-linear model, we find strong evidence for three distinct regimes, each with markedly different reactions from safe-haven and high-yielding currencies involved in speculative carry trades. While the first and third regimes correspond to high carry trade intensity depending on the currency's role in the carry trade, the second regime represents an indeterminate region. It accounts for the uncertainty in the threshold variable when discriminating between different intensities of carry trade activity. It also captures potential shifts in the purpose of a currency in the carry trade – from a funding currency to an investment currency, or vice versa – reflecting the time needed to adjust investment strategies. In general, carry trade activity is capable to change the transmission of monetary policy. It is important to distinguish whether the foreign currency is used as a funding (safe-haven currencies) or investment currency (high-yielding currencies). A contractionary monetary policy shock makes the carry trade more (less) attractive for safe-haven (high-yielding) currencies. For these groups, we observe similar dynamics in the high carry trade intensity regime. We summarize the results as follows. First, higher carry trade activity leads to larger excess returns where the adjustment mainly happens through the interest rate differential. Second, we only find mild differences for exchange rates across regimes. As in the linear case, results show an appreciation (depreciation) to the monetary policy (central bank information) shock.[3] Third, these findings hold for both shocks and currency sets. Fourth, by investigating the responses of risk aversion, our results show that these are not the driving force of the effects but it suggests that speculative trading is important. Fifth, when looking closer at the responses of risk aversion, this channel is more muted for monetary policy shocks than for central bank information shocks. Our results from the non-linear model thus strongly support the notion of currency speculation as an amplifier of monetary policy transmission.

We also develop an FX trading strategy to consider the impact of U.S. monetary policy shocks on various currency risk premia and excess returns in currency speculation (Cieslak, Morse and Vissing-Jorgensen, 2019; Brusa, Savor and Wilson, 2020; Mueller, Tahbaz-Salehi and Vedolin, 2017; Falconio, 2023). Our strategy

[3] Again, we find that an appreciation of the U.S. dollar in the group of safe-haven currencies to the central bank information shocks.

involves trading on the day of central bank announcements and explicitly accounts for the co-movement of interest rate and stock price surprises. It strongly outperforms a strategy that ignores information released on monetary policy announcement days and trades only at the end of the month, as well as one that does not differentiate between the types of shocks. The strategy demonstrates notable improvements in both the Sharpe ratio and skewness. Additionally, cumulative return calculations show that it effectively protects the portfolio from large losses, which are typically a risk with conventional currency trading strategies.

The remainder of the paper is structured as follows. In the following section, we discuss our contribution to the related literature. In section 3 we provide some motivating evidence on the relation between monetary policy shocks and exchange rate dynamics. Furthermore, we discuss the underlying theoretical model and the carry trade indicator for our non-linear model. Section 4 discusses the econometric model and the empirical results both from the linear and non-linear specification, while section 5 presents our trading strategy. Finally, section 6 concludes.

2 Related Literature

We contribute to the literature on how U.S. monetary policy and central bank information shocks affect foreign exchange markets vis-à-vis the U.S. dollar. We rely on a cash-flow-based model of exchange rates and link currency carry trade activity to the two types of monetary policy shocks. This allows us to examine how the transmission to these shocks alters exchange rates, excess returns, and crash risk. Finally, we utilize information around Federal Open Market Committee (FOMC) announcements in a trading exercise, outperforming the carry trade strategy in terms of the Sharpe ratio and downside risk. In the following we outline the four key contributions to the literature on exchange rate dynamics.

First, we demonstrate that the nature of monetary policy shocks is critical in determining how exchange rates respond. A large and robust literature has documented that a standard monetary tightening leads to an appreciation of the domestic currency.[4] However, central bank decisions may also convey other information not reflected in the realm of "traditional" monetary policy with potentially different effects on exchange rates (Nakamura and Steinsson, 2018). Jarociński and Karadi (2020) confirm the importance of distinguishing the nature of the shock by exploiting the stock price reaction in addition to the interest rate reaction around policy announcements, arguing the presence of *information* effects. Similarly, Cieslak and Schrimpf (2019) analyze asset price changes on policy announcement dates based on the co-movement of stock and bond yields. They show that central bank announcements not only convey aspects of monetary policy, but also on economic growth and risk premium news, which are likely drivers of asset prices.[5] Closely related to this is Pinchetti and Szczepaniak (2023) who find for a panel of developed and emerging market currencies a depreciation of the U.S. dollar to an information shock. They relate this result to an increase in investors' risk appetite, which squares with findings of Stavrakeva and Tang (2019). However, this phenomenon appears

[4] See, inter alia, Kim and Roubini (2000), Favero and Marcellino (2001), Faust et al. (2007), Degasperi, Hong and Ricco (2020) and Boeck and Mori (2023).

[5] Recently, Aruoba and Drechsel (2024) used natural language processing methods on publicly available Fed policy documents to show that, prior to policy decisions, these documents capture essential economic information not reflected in staff forecasts. For unconventional monetary policy tools, Lunsford (2018) also provides similar evidence, relating it to investors' repricing of output and inflation expectations. This confirms the existence of additional shocks not incorporated in standard monetary policy shocks.

to be currency-specific (Franz, 2020). We contribute to this literature two insights. First, we corroborate the findings of different exchange rate adjustment mechanisms to different monetary policy actions in a large cross-country setting (and highlight currency idiosyncrasies). Second, we extend this analysis to take speculative carry trade activity in a non-linear fashion into account.

Second, we relate to unique characteristics of currencies that make them susceptible to speculation, reflected in deviations from the assumption of Gaussianity. Sudden and unexpected exchange rate reactions can occur in conjunction with or as a result of financial shocks, which is particularly prevalent in high-yielding currencies. Here, currency crashes are explained by risk-based approaches (see among others Brunnermeier, Nagel and Pedersen, 2008; Ang and Chen, 2010; Della Corte, Riddiough and Sarno, 2016; Menkhoff et al., 2017) or behavioral approaches such as herding behavior in foreign exchange markets (for example, Frankel, Froot et al., 1986; Sokolovski, 2007; De Grauwe and Kaltwasser, 2012; Hasselgren, 2020). Within this strand of literature, the currency carry trade strategy stands out. By exploiting the interest rate differential between two currencies, it is able to generate significant excess returns (see, inter alia, Burnside et al., 2006; Lustig, Roussanov and Verdelhan, 2011; Mueller, Tahbaz-Salehi and Vedolin, 2017; Falconio, 2023). This specific strategy is associated with the creation of bubbles and high crash risks (see, e.g., Plantin and Shin, 2006; Kaizoji, 2010; Spronk, Verschoor and Zwinkels, 2013). As Sokolovski (2007) argues, during periods of high carry trade activity – or "crowdedness" – large negative interest rate shocks force carry traders to unwind their positions to avoid a loss. Ultimately, if the mass of traders following this strategy is large enough, the exchange rate can suddenly depreciate sharply also pointing towards non-linearities (Plantin and Shin, 2006). To distinguish hedging from speculative motives Brunnermeier, Nagel and Pedersen (2008) operationalize futures position data to construct a measure of carry trade activity. Their finding suggests that carry trade activity is indeed an important determinant for enhanced currency volatility and currency crash risks. In contrast, we contribute to this literature by distinguishing not only monetary policy and information shocks but also by incorporating speculative currency trading in our analysis.

Third, as we develop a trading strategy based on these insights, we align with Mueller, Tahbaz-Salehi and Vedolin (2017) and Falconio (2023), who find that currency returns are higher on the days of monetary policy announcements. While the former argues that higher returns compensate for elevated monetary policy uncertainty, the latter attributes the increase to future real interest rate differentials driving higher returns of this strategy. Additionally, Zviadadze (2017) shows that macroeconomic risks significantly influence the term structure of carry returns. Our developed strategy thus contributes to the literature by explicitly incorporating the different nature of Fed surprises originating from monetary policy announcements.

Finally, our analysis relies on a cash-flow based convenience yield concept, based on Jiang, Lustig and Krishnamurthy (2021) extending Campbell and Clarida (1987) and Clarida and Gali (1994). It incorporates the idea that in times of financial distress or uncertainty, U.S. assets are in high demand as they are safe and liquid (see among others Chahrour and Valchev, 2018; Du, Im and Schreger, 2018; Gopinath and Stein, 2021) thus earning a *convenience yield*. Furthermore, the U.S. dollar is an important reserve and invoicing currency (Goldberg and Tille, 2009) and second, the U.S. economy and its central bank are key drivers of the global financial cycle (Miranda-Agrippino and Rey, 2020). Thus, the U.S.dollar is seen to enjoy an "exorbitant privilege" (Gourinchas and Rey, 2007), which this underlying model takes properly into account.

3 Exchange Rates, Monetary Policy, and Currency Carry Trade

In this section, we present some motivating evidence for the subsequent analysis. First, the nature of monetary policy surprises determine the reaction of the exchange rate. Second, the reactions are heterogeneous across currencies pointing towards currency-specific aspects. We address these by introducing a cash-flow based view on exchange rate dynamics following Jiang, Lustig and Krishnamurthy (2021). Third, the exchange rate market is not only influenced by macro fundamentals but given the presence of interest rate differentials also subject to speculative trading. We examine the currency carry trade strategy and how it relates to monetary policy and interest rate differentials. This strategy exploits interest rate differentials, by investing in currencies with high interest rates and funding in low interest rate currencies. Monetary policy affects these interest rate differentials and thus the risk profile of this strategy, making it pivotal for exchange rate dynamics.

Our paper studies the connection between these aspects with a set of 15 currencies against the U.S. dollar. The set of currencies consists of 9 developed market (DM) economies and 6 emerging market (EM) economies with floating exchange rates: Australian dollar (AUD), Canadian dollar (CAD), Swiss franc (CHF), Czech koruna (CZK), the Euro (EUR), Pound sterling (GBP), Indian rupee (INR), Japanese yen (JPY), Mexican peso (MXN), Norwegian krone (NOK), New Zealand dollar (NZD), Philippine peso (PHP), Swedish krona (SEK), Thai baht (THB), and the South African rand (ZAR). All currencies are expressed per unit of the U.S. dollar, i.e., an increase in the spot exchange rate indicates an appreciation of the U.S. dollar. This dataset constitutes a monthly unbalanced panel but we have ensured that all starting dates are before 2000 (except for the Czech koruna and the Thai baht, which start in November 2000 and January 2002, respectively). An overview of the data sources and the sample is provided in App. A.

An overview on the currencies is given in Tab. 1, where we report summary statistics of, inter alia, monthly currency excess returns (annualized and in percent) and forward discounts. Since market interest rates are for certain currencies only available with a maturity of three month, we define the currency excess returns as follows. An investor buys a foreign currency i in the forward market and sells the U.S. dollar in the spot market after three months such that $rx_{it+3} = f_{it}^{3m} - s_{it+3}$. Under the assumption of the covered interest rate parity, the log forward discount, $f_{it}^{3m} - s_{it}$ should be equal to the interest rate differential between the foreign and US interest rate, $i_{it}^{*} - i_{t}^{\$}$. Hence, we can define the currency excess return for currency i also as

$$rx_{it+3} = i_{it}^{*} - i_{t}^{\$} - (s_{it+3} - s_{it}) = i_{it}^{*} - i_{t}^{\$} - \Delta s_{it+3}. \tag{3.1}$$

The summary statistics reveal that excess returns of emerging market currencies as well as AUD, NOK, and NZD show higher standard deviations, a positive mean and are strongly negatively skewed often accompanied with large kurtosis. This indicates the presence of extreme events in the data, resulting in fat tails. Low-yielding currencies, such as JPY and CHF, exhibit positive skewness in excess returns. This behavior, along with their correlation with risk aversion, supports their classification as *safe-haven* currencies (Ranaldo and Söderlind, 2010; Habib and Stracca, 2012). The summary statistics also point to the fact that some currencies are prone to sharp sudden depreciations, given the negative skeweness and leptokurtic characteristics of the excess returns (Brunnermeier, Nagel and Pedersen, 2008).

Table 1: Summary Statistics of Currency Returns.

Currency	Mean	SD	Skewness	Kurtosis	FD/P	NOI	TB
AUD	1.13	12.58	−0.76	7.07	0.45	0.12	0.00
CAD	−0.05	8.07	−0.13	5.39	0.00	0.02	−0.20
CHF	0.25	10.74	0.06	3.10	−0.28	−0.09	−0.38
CZK	2.34	12.36	−0.21	3.47	−0.11		−0.59
EUR	−0.76	9.60	−0.26	3.58	−0.23	0.06	−0.19
GBP	0.33	9.85	−0.94	7.25	0.30	−0.01	0.03
INR	2.14	7.37	−0.98	5.50	1.13		−1.82
JPY	−3.34	11.19	0.31	3.91	−0.61	−0.12	−0.43
MXN	2.81	10.94	−0.96	5.87	1.71		−0.09
NOK	0.64	11.09	−0.57	5.66	0.19		−0.16
NZD	2.47	11.40	−0.21	4.56	0.60	0.21	−0.01
PHP	0.69	8.84	−1.15	8.17	0.94		−0.75
SEK	−0.85	11.15	−0.41	4.52	−0.01		−0.18
THB	2.76	6.20	−0.33	2.75	0.22		−0.21
ZAR	1.98	16.41	−0.10	4.23	1.55		−0.20

Notes: This table shows summary statistics (averages) of the currencies in the sample. The table reports the annualized mean and standard deviation (SD) in percent, as well as skeweness and kurtosis of log excess 3-month returns, $rx_{t+3} = f_{it}^{3m} - s_{it+3}$ for currency i, which is the difference between the log spot rate in three month, s_{it+3}, and the 3-month log forward rate, f_{it}^{3m}. $f_{it}^{3m} - s_{it}$ is the forward discount/premium (FD/P) in percent, defined as the difference of the 3-month log forward and log spot rate. NOI represents the net open interest, NOI_{it}. The last column reports the one year Treasury basis (TB), calculated according to Eq. (3.4) in percentage points.

3.1 Exchange Rates and Monetary Policy Shocks

To explore factors behind non-normality of currency returns, we provide suggestive evidence that exchange rates reactions depend on the nature of a monetary policy surprise. We measure unanticipated U.S. monetary policy surprises via high-frequency proxies.[6] These high-frequency proxies are price changes of interest rate derivatives in a narrow window surrounding FOMC monetary policy announcements and labeled as *surprises*.[7] These changes then reflect the exogenous changes in expectations solely due to the announcement of the new and unanticipated monetary policy stance. Following Jarociński and Karadi (2020), we use high-frequency surprises in interest rate derivatives and in the S&P 500 stock market index to differentiate between monetary policy and central bank information shocks.[8] A shock is denoted as *monetary policy shock*, MP_t, if the high-frequency surprises on the interest rate derivatives and the stock market co-move negatively. On the contrary, a positive co-movement between these high-frequency surprises constitutes a *central bank information shock*, CBI_t.[9]

[6] This builds upon a large literature, see, inter alia, Kuttner (2001), Gürkaynak, Sack and Swanson (2005), Gertler and Karadi (2015), Nakamura and Steinsson (2018), Jarociński and Karadi (2020), Miranda-Agrippino and Ricco (2021) and Bauer and Swanson (2023b).

[7] This window is defined as 10 minutes before and 20 minutes after the announcement and rules out potential confounding factors.

[8] We follow the methodology in Jarociński and Karadi (2020) to construct the surprises in the interest rate derivatives. These are constructed as the first principal component of five high-frequency surprises: the current-month Fed funds future, the 3-month Fed funds future, and the eurodollar futures at the horizons of two, three, and four quarters, respectively. The advantage of this procedure is that it partly also captures unconventional monetary measures, like forward guidance. We obtained the data via `https://marekjarocinski.github.io/jkshocks/jkshocks.html`.

[9] This simple decomposition is also dubbed "poor man's sign restrictions" in Jarociński and Karadi (2020).

Figure 1: Average Spot Reactions to Monetary Policy and Central Bank Information Shocks.

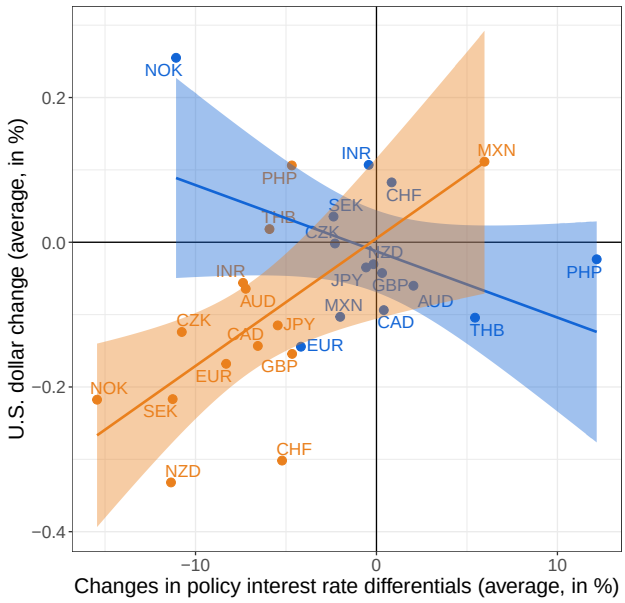

Notes: The figure reports the weighted-average change of the U.S. dollar against a subset of currencies (in %) alongside the changes in the policy interest rate differentials relative to the U.S. ($pir^* - pir^{US}$) following FOMC meetings with a restrictive monetary policy decision. Points highlighted in blue indicate a meeting with a monetary policy surprise, while those in orange represent meetings with a central bank information surprise. For the former (latter) we consider FOMC meetings from 2000 (2003) until 2018. ZAR has been excluded as an outlier. Negative changes in the policy rate indicate an increase of the U.S. policy rate and positive changes of the U.S. dollar change are an appreciation.

In terms of exchange rates and interest rates, we collect daily spot and policy rates at the day before and on the day of the policy announcements of the FOMC, respectively, and compute the changes.[10] For this analysis, we construct two subsets of the surprises. The first subset is based on a negative co-movement between interest rate and stock market surprises (resulting in a monetary policy shock), while the second subset is based on a positive co-movement (the central bank information shock). We focus on shocks that are associated with an interest rate increase and consider FOMC meetings from 2000 until 2018. To account for the different shock magnitudes, we proceed with a construction of simple weights for each shock by dividing the MP_t (CBI_t) component on date t by the sum of all MP (CBI) shocks. Hence, the weight for an MP (CBI) shock occurred on date t can be written as: $w_t^{MP} = \frac{MP_t}{\sum MP}$ ($w_t^{CBI} = \frac{CBI_t}{\sum CBI}$), where $\sum MP$ ($\sum CBI$) represents the sum of all shocks over the observed period. Finally, we calculate the weighted mean of all spot rate changes as $\sum w_t^j \cdot \Delta s_t$ ($j \in \{MP, CBI\}$) for each currency.

In Fig. 1 we plot the weighted mean of all spot rate changes on the weighted mean of changes in the policy interest rate differential ($pir^* - pir^{US}$) for both types of shocks. First, this analysis reveals that, on average, stronger policy rate changes are associated with larger changes in the U.S. dollar (USD) exchange rate. Second, the nature of the underlying shock determines the direction of the change of the U.S. dollar exchange rate. An increase in the U.S. policy rate due to a monetary policy shock indicates a negative change

[10]For an overview of the data, see App. A.

Figure 2: Response of Currencies vis-à-vis the U.S. Dollar to Monetary Policy and Information Shocks.

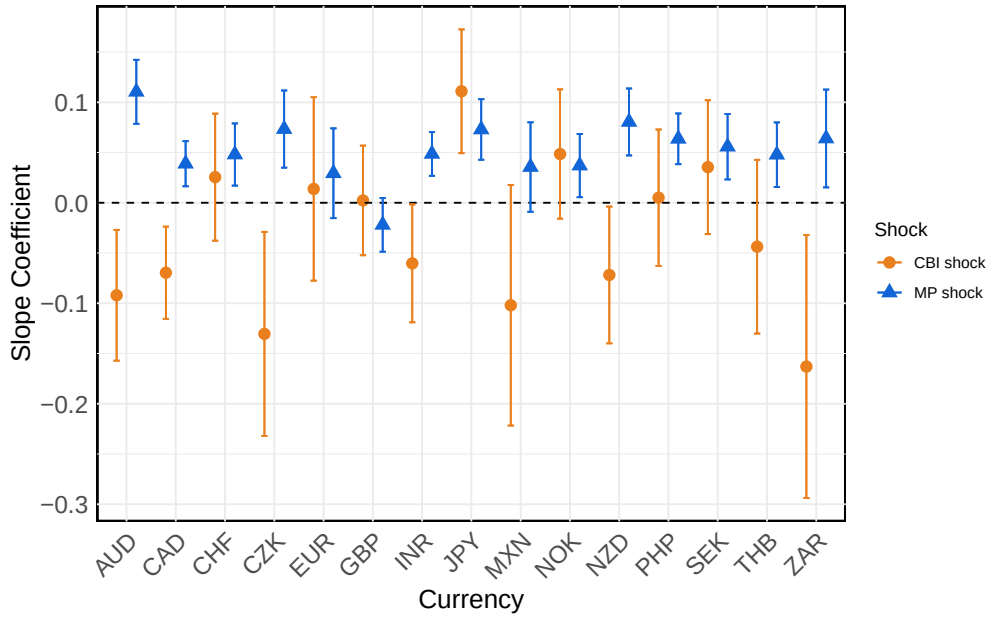

Notes: The figure shows the point estimates and the respective standard errors of β_{MP}, in blue, and β_{CBI}, in orange, of Eq. (3.2).

in the differential and leads to a positive change in the USD (blue line). This reflects an appreciation of USD – the standard reaction to a contractionary monetary policy shock. However, if the interest rate increase is associated with surprising information about the state of the economy, the relationship deviates from previous evidence. In this case, the U.S. dollar depreciates against other currencies on average (orange line).

In a next step, we examine individual currency reactions to monetary policy and central bank information shocks originating from the Federal Reserve. For that, we aggregate these intraday surprises up to a monthly frequency. If in month t more than one FOMC announcement takes place, we add up all intraday surprises occurring in month t. If there are no FOMC announcements in month t, we set the surprises equal to zero. We estimate the following regression for each currency in our sample

$$\Delta s_t = \beta_{cons} + \beta_{MP} MP_t + \beta_{CBI} CBI_t + \varepsilon_t, \tag{3.2}$$

where Δs_t denotes the respective spot rate change, MP_t and CBI_t the respective shocks defined above, and ε_t a Gaussian error term.

In Fig. 2 we report the point estimates of β_{MP} and β_{CBI} together with their respective standard errors. A clear picture emerges, as surprises stemming from (contractionary) monetary policy typically lead to a positive coefficient, indicating an appreciation of the U.S. dollar, confirming previous evidence. A central bank information surprise, on the other hand, is mostly associated with a depreciation of the U.S. dollar against most currencies. This confirms the results of Pinchetti and Szczepaniak (2023), who additionally provide panel data evidence for developed and emerging market currencies separately. However, we find that some currencies do not react statistically significantly differently to the two shocks, while others show large significant differences. In general, the estimates for the central bank information shock show much more

uncertainty, while the estimates associated with the monetary policy shock are more precise. We observe a considerable amount of heterogeneity in the responses between currencies typically associated with high or low yields. We observe different signs of the (large) responses to the respective shocks for high-yielding developed market currencies, such as the Australian, Canadian, and New Zealand dollar, and for emerging market currencies. Results for the low-yielding currencies (such as the Swiss franc, the Euro and the British pound) do not show different effects on the two shocks in this regression. For the Japanese yen the results suggest both shocks (although not statistically different) lead to a depreciation against the U.S. dollar. The results suggest that the difference in currency response can be attributed to specific characteristics, such as risk levels and yield profiles. In what follows, we relate these results to the exposure of the respective currencies to a specific trading strategy, the currency carry trade.

3.2 Modeling Exchange Rates

To establish a connection between exchange rate dynamics and monetary policy for our consecutive analysis, we rely on the exchange rate model developed by Jiang, Lustig and Krishnamurthy (2021), which provides a cash-flow based view. This model builds on the observation that investors around the globe demand U.S. dollar assets as safe assets, and are thus willing to forgo some return to own these assets. This forgone return is called *convenience yield* and can explain a sizeable share of exchange rate fluctuations. Based on a microfounded model, they show that the level of the nominal U.S. dollar exchange rate can be written as the sum of future convenience yield differences, the sum of interest rate differences, and the sum of the currency risk premia as well as a constant, which then reads

$$s_t = \mathbb{E}_t \sum_{\tau=0}^{\infty} (\lambda^{\$,*}_{t+\tau} - \lambda^{*,*}_{t+\tau}) + \mathbb{E}_t \sum_{\tau=0}^{\infty} (y^{\$}_{t+\tau} - y^{*}_{t+\tau}) - \mathbb{E}_t \sum_{\tau=0}^{\infty} rp^{*}_{t+\tau} + \bar{s}. \tag{3.3}$$

In this equation, s_t is the logarithm of the spot rate expressed in foreign currency per unit of the U.S. dollar, $\lambda^{\$,*}_t - \lambda^{*,*}_t$ is the difference between the convenience yield of the foreign investor for the investment in U.S. Treasury bonds and the convenience yield for the investment in the foreign bonds, and $y^{\$}_t - y^{*}_t$ is the difference in the U.S. and foreign government bond yields. Lastly, rp^{*}_t is the realized risk premium earned by the foreign investor for buying U.S. safe assets. The term $\bar{s}$ is the average of the nominal spot exchange rate, which is assumed to be stationary.

However, both the convenience yield and the risk premium are latent quantities, which according to Jiang, Lustig and Krishnamurthy (2021) can be inferred from the *treasury basis*, x^{Treas}_t. This is the difference between the yield on U.S. Treasuries, $y^{\$}_t$, and a synthetic dollar yield of a foreign government bond, which earns a yield y^{*}_t in foreign currency and is then hedged back into dollars. It is defined as follows

$$x^{Treas}_t \equiv (y^{\$}_t - y^{*}_t) + (f^{1}_t - s_t), \tag{3.4}$$

where f^{1}_t and s_t are the logarithm of the one-year forward rate and the logarithm of the spot exchange rate, while $y^{\$}_t$ and y^{*}_t are U.S. and foreign one-year government bond yields, respectively. A negative treasury basis implies that U.S. Treasuries are more expensive compared to foreign ones. Given this notion, the treasury

basis can be used to infer the convenience yield by

$$\lambda_t^{\$,*} - \lambda_t^{*,*} = -\frac{x_t^{Treas}}{1-\beta^*}, \tag{3.5}$$

where the proportionality factor depends upon a constant, $0 < \beta^* < 1$. This constant indicates the foreign investor's preference for a synthetically created dollar deposit relative to the U.S. Treasury investment. A $\beta^* = 0$ would imply that U.S. Treasuries create no additional benefit in terms of convenience yields, which then can be dubbed as *dollarness*. On the contrary, if β^* approaches unity, investors start appreciating the safety and liquidity of U.S. assets, which get thus more expensive. Hence, in the latter case, we observe a convenience yield. Jiang, Lustig and Krishnamurthy (2021) estimate a $\beta^* = 0.90$ and therefore conclude that there is indeed a convenience yield attached to U.S. Treasuries. For our sample, the average Treasury basis is negative for all currencies except for the Australian dollar ($x_t^{Treas} = 0$) and the Pound sterling ($x_t^{Treas} = 0.03$), as seen in Tab. 1. That means, U.S. Treasuries are more expensive compared to treasuries from other countries in our sample, except two. Especially, emerging market currencies, like INR and PHP reveal a strongly negative Treasury basis.

The *risk premium* can be expressed as the log excess return minus the convenience yield, i.e.,

$$rp_t^* = rx_t - \frac{1}{1-\beta^*} x_{t-1}^{Treas}. \tag{3.6}$$

The log currency excess return earned from the long position in the foreign currency is the interest rate differential less the rate of depreciation, as defined in the equation for the currency excess return in Eq. (3.1).

The model proposed by Jiang, Lustig and Krishnamurthy (2021) shows the importance of the treasury basis for exchange rate dynamics from a cash flow perspective. For our purpose, it allows us to link exchange rate dynamics to interest rate movements directly through the interest rate differential and indirectly through the convenience yield. Furthermore, it enables us to establish the connection to speculative currency trading, which is the main contribution of the paper.

3.3 Carry Trade Activity and Monetary Policy

As we are interested in how carry trade activity influences the relation between monetary policy and foreign exchange markets, we need a measure of carry trade activity. Given that the interest rate differential serves as a signal for creating a carry trade strategy, it naturally emerges as a suitable measure of carry trade activity.[11] However, it neither measures *actual* trades nor discriminates between hedging and speculative motives, which are important features for the consecutive analysis. Therefore, we resort to the proxy of carry trade activity against the U.S. dollars provided in Brunnermeier, Nagel and Pedersen (2008), who introduce the *net open interest*, NOI_{it} for a selected set of currencies in our sample. For the construction of this variable, we

[11] A rather standard measure is also the forward discount, the difference between a forward and the corresponding spot rate as, for instance, used in Burnside, Eichenbaum and Rebelo (2007) and Burnside, Eichenbaum and Rebelo (2011).

Figure 3: Net Open Interest and the Policy Interest Rate Differential.

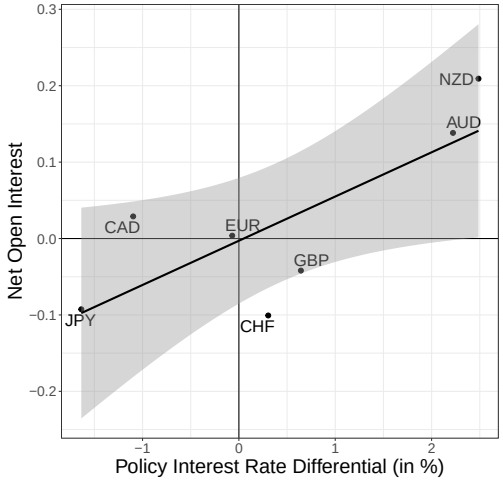

Notes: The figure presents the relationship between the average net open interest in the foreign exchange futures markets and the average policy interest rate differentials relative to the U.S. ($pir^* - pir^{US}$). Net open interest is calculated as the difference between the long and short futures positions of noncommercial traders divided by the total open interest. A point indicates the average interest rate differential and the average net open interest over the sample from 2000M05 to 2019M12.

rely on the currency futures positions of the U.S. Commodity Futures Trading Commission (CFTC).[12] It distinguish between *commercial* and *non-commercial* traders. According to the definition of the CFTC, the non-commercial traders use futures not for hedging purposes. This implies that they are using these futures for speculative reasons. To gather the elevated activity in the foreign currency with respect to the U.S. dollar, we calculate the *net* open interest. It is represented as the difference between the long and short futures positions of non-commercial traders divided by the total open interest, such that

$$NOI_{it} = \frac{\text{Long}_{it} - \text{Short}_{it}}{\text{Total Open Interest}_{it}}. \tag{3.7}$$

The greater the absolute value of the net open interest, the higher the probability that the foreign currency is exposed to speculative currency carry trading activity. Moreover, the sign provides another important information. A positive NOI_{it} means that investors predominantly sell the U.S. dollar and buy the foreign currency i, using the foreign currency as an *investment*. On the contrary, a negative NOI_{it} indicates that investors buy the U.S. dollar and sell the foreign currency, using it as a *funding* currency. As net open interest rises, investors are increasingly viewing the currency as a favorable investment, allocating more capital to it. The implementation of the simple carry trade strategy may systematically generate excess returns, especially if the interest differential is large.

To highlight this link, in Fig. 3 we plot the average policy interest rate differential from 2000M05 to 2019M12 against the average net open interest. Together with the summary statistics in Tab. 1, we conclude that typical low-yielding currencies like JPY and CHF with a negative or very low interest rate differential to

[12]We gathered the Commitments of Traders (COT) reports that offer a breakdown of open interest for both futures contracts. It provides the positions maintained by various categories of traders. The CFTC data are initially reported on a weekly basis, where we use the end-of-month vintages.

the US, show a negative net open interest. On the contrary, high-yielding currencies, such as MXN, NZD, or AUD offer large differentials and a pronounced positive NOI_{it}. The greater the interest rate differential in absolute values, the higher is the NOI_{it}, indicating a pronounced speculative carry trading activity. The established link motivates our identification of different currency regimes later on.

The summary statistics also reveal a positive correlation (0.69) between the average forward discount/premium and the average net open interest. Also the correlation between the average returns as well as the average treasury basis and the average NOI is positive (0.83 and 0.72, respectively). Finally, a negative correlation (-0.49) between currency skewness and the net open interest confirms the evidence in the existing literature that carry trade activity may be associated with a higher probability of currency crashes (Brunnermeier, Nagel and Pedersen, 2008).

4 Empirical Evidence

In this section, we proceed to modeling exchange rate dynamics and monetary policy jointly in a multivariate non-linear empirical framework. The analysis distinguishes between monetary policy and central bank information shocks in the analysis. We introduce our econometric framework, before we present the results. First, we discuss the evidence from the linear model before we move to the non-linear threshold model, and conclude with a robustness assessment.

4.1 Econometric Framework

We build upon the econometric framework of Jarociński and Karadi (2020). For a general exposition of the framework, let $\{\boldsymbol{y}_{it}\}_{t=1}^{T}$ denote an $n_y \times 1$ vector of endogenous macroeconomic and financial variables at a monthly frequency and let $\{\boldsymbol{m}_t\}_{t=1}^{T}$ be an $n_m \times 1$ vector of exogenous high-frequency instruments aggregated to a monthly frequency. In our specific empirical setting, we have an unbalanced panel of countries ($i = 1, \ldots, N$) with $n_y = 4$ with $\boldsymbol{y}_{it} = (i_t^{\$}, i_{it}^{*}, x_{it}^{Treas}, s_{it})'$, where $i_t^{\$}$ is the U.S. interest rate and i_{it}^{*} its foreign counterpart, x_{it}^{Treas} the treasury basis, and s_{it} the exchange rate for currency i. The $n_m = 2$ proxies, $\boldsymbol{m}_t = (m_t^{\text{fff}}, m_t^{\text{SP500}})'$, denote high-frequency movements aggregated at a monthly frequency in policy-relevant interest rate derivatives and in the S&P500 stock market index, respectively.

We gather all variables at a monthly frequency in the $n \times 1$ vector $\boldsymbol{Y}_{it} = \left(\boldsymbol{m}_t', \boldsymbol{y}_{it}'\right)'$. Then the linear specification reads as follows

$$\underbrace{\begin{pmatrix}\boldsymbol{m}_t\\ \boldsymbol{y}_{it}\end{pmatrix}}_{=\boldsymbol{Y}_{it}} = \underbrace{\begin{pmatrix}\boldsymbol{0}\\ \boldsymbol{c}_i^{y}\end{pmatrix}}_{=\boldsymbol{c}_i} + \sum_{j=1}^{p} \underbrace{\begin{pmatrix}\boldsymbol{0} & \boldsymbol{0}\\ \boldsymbol{A}_{ij}^{my} & \boldsymbol{A}_{ij}^{yy}\end{pmatrix}}_{=\boldsymbol{A}_{ij}} \underbrace{\begin{pmatrix}\boldsymbol{m}_{t-j}\\ \boldsymbol{y}_{it-j}\end{pmatrix}}_{=\boldsymbol{Y}_{it-j}} + \underbrace{\begin{pmatrix}\boldsymbol{\varepsilon}_t^{m}\\ \boldsymbol{\varepsilon}_{it}^{y}\end{pmatrix}}_{=\boldsymbol{\varepsilon}_{it}}, \qquad \boldsymbol{\varepsilon}_{it} \sim \mathcal{N}\left(\boldsymbol{0}, \boldsymbol{\Sigma}_i\right), \tag{4.1}$$

where $\boldsymbol{c}_i^{y}$ denotes the $n_y \times 1$ vector of constants, $\boldsymbol{A}_{ij}^{yy}$ is the $n_y \times n_y$ matrix of coefficients for lag j, $\boldsymbol{A}_{ij}^{my}$ denotes an $n_m \times n_y$ matrix of coefficients, and $\boldsymbol{\Sigma}$ is an $n \times n$ variance-covariance matrix. We assume that the surprises in $\boldsymbol{m}_t$ have zero mean and do not depend on any lags of endogenous variables. These restrictions are plausible as long as the financial market surprises are unpredictable. We estimate this model for each currency i separately.

For the non-linear version of the model, we utilize a threshold approach. We keep the parametric restrictions on $\boldsymbol{c}_i$ and $\boldsymbol{A}_{ij}$ in each regime. We allow for three regimes, which are distinguished by the lagged net open interest, NOI_{it}, the threshold variable. We use the first lag of the MA(5)-smoothed net open interest for currency i to account for delays in the adjustment process. The threshold model with three regimes indicated by $r \in \{1, 2, 3\}$ for a specific currency i reads as follows

$$\boldsymbol{Y}_{it} = \begin{cases} \boldsymbol{c}_{1i} + \sum_{j=1}^{p} \boldsymbol{A}_{1,ij} \boldsymbol{Y}_{it-j} + \boldsymbol{\varepsilon}_{it}, & \boldsymbol{\varepsilon}_t \sim \mathcal{N}(\boldsymbol{0}, \boldsymbol{\Sigma}_{1i}) \qquad \text{if } -\infty < NOI_{it-1} \leq \gamma_{1i}, \\ \boldsymbol{c}_{2i} + \sum_{j=1}^{p} \boldsymbol{A}_{2,ij} \boldsymbol{Y}_{it-j} + \boldsymbol{\varepsilon}_{it}, & \boldsymbol{\varepsilon}_t \sim \mathcal{N}(\boldsymbol{0}, \boldsymbol{\Sigma}_{2i}) \qquad \text{if } \gamma_1 < NOI_{it-1} \leq \gamma_{2i}, \\ \boldsymbol{c}_{3i} + \sum_{j=1}^{p} \boldsymbol{A}_{3,ij} \boldsymbol{Y}_{it-j} + \boldsymbol{\varepsilon}_{it}, & \boldsymbol{\varepsilon}_t \sim \mathcal{N}(\boldsymbol{0}, \boldsymbol{\Sigma}_{3i}) \qquad \text{if } \gamma_2 < NOI_{it-1} < \infty, \end{cases} \tag{4.2}$$

where $\boldsymbol{c}_{ri}$ $(r = 1, 2, 3)$ is an $n \times 1$ regime-specific constant, $\boldsymbol{A}_{r,ij}$ an $n \times n$ regime-specific coefficient matrix for lag j, and $\boldsymbol{\Sigma}_{ri}$ an $n \times n$ regime-specific variance-covariance matrix. Again, we estimate the model for each currency i separately.

In our application with monthly data, we set the number of lags to $p = 2$ to sufficiently account for dynamics.[13] We follow Jarociński and Karadi (2020) for the identification of the monetary policy shock and central bank information shock and use sign restrictions on the proxies. For the monetary policy shock, we induce a negative co-movement between the two proxies. On the contrary, for the central bank information shock we assume a positive co-movement of the interest rate derivative and stock market surprises. Additionally, we impose a positive sign on the U.S. interest rate to ensure a rise in the U.S. interest rate across all currency models. Sign restrictions are implemented using the algorithm outlined in Rubio-Ramírez, Waggoner and Zha (2010). For that, we assume a uniform prior on the space of rotations conditionally on satisfying the imposed sign restrictions. This yields then a set-identified semi-structural (non-)linear model.

The model is estimated using Bayesian techniques as in Chen and Lee (1995) and Boeck and Zörner (2024). We assume the horseshoe shrinkage prior for the VAR coefficients (Carvalho, Polson and Scott, 2010) and an inverse-Wishart prior for the covariance matrices and draw all parameters through Markov Chain Monte Carlo integration. For more details on the prior specification, we refer to App. B. We sample 35,000 draws from the posterior distribution, where we discard the first 10,000 and use a thinning factor of two on the remaining draws. This leaves us with 12,500 draws for the posterior analysis. We also report average responses across all of the currencies or specific currency groups in our sample. The average coefficient estimates are given by $\boldsymbol{\theta} = \sum_{i=1}^{N} \boldsymbol{\theta}_i / N$ for $i = 1, \ldots, N$, where $\boldsymbol{\theta}_i$ denotes the vector of all coefficients of the model of currency i. We compute impulse responses using this average estimates and interpret them as an average currency response within this group. This procedure yields the same regression coefficients as averaging currency-by-currency estimates, as proposed by Pesaran and Smith (1995).

4.2 Evidence from the Linear VAR Model

Fig. 4 shows impulse response functions to a contractionary monetary policy shock (upper panel) and central bank information shock (lower panel). We report the impulse responses of the group-mean estimator of the

[13] Information criteria such as the BIC or AIC point to a low number of lags. Adding more lags increases the number of parameters to be estimated substantially, such that the precision suffers. However, the results do not change qualitatively for lags up to six months.

Figure 4: Impulse Responses of the Baseline Model.

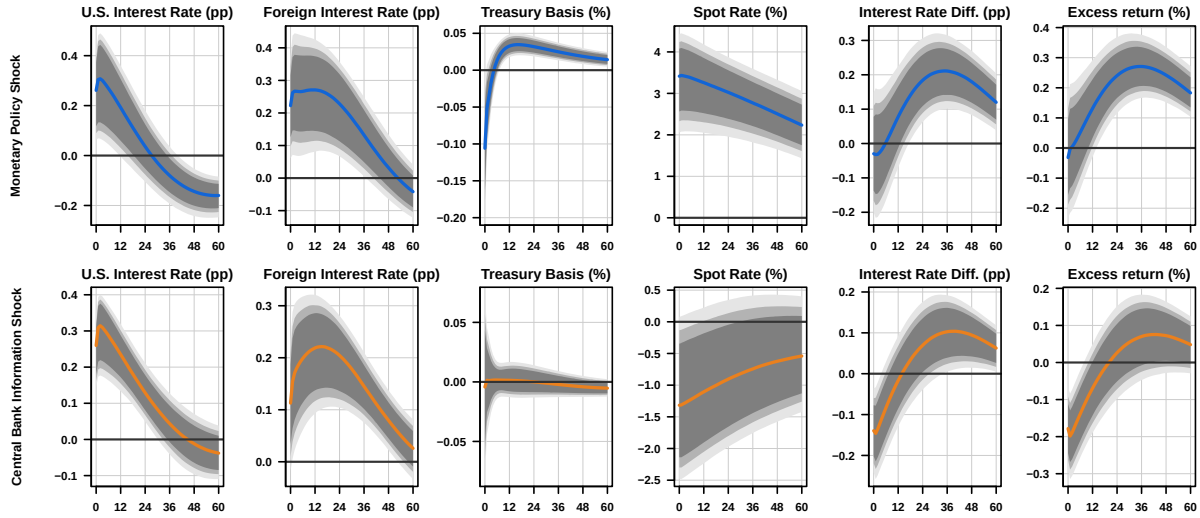

Notes: The upper panel shows the impulse responses to the U.S. monetary policy shock, while the lower panel shows the impulse responses to the central bank information shock. Estimation is based on the group-mean estimator of the linear VAR model. Solid lines represent posterior median estimates, shaded areas indicate 68/80/90 percent credible sets. Horizontal axis measures time in months. Vertical axis measures deviation from pre-shock level in percent (%) or percentage points (pp).

single-currency VAR models. The shock is normalized such that the the U.S. interest rate increases by 25 basis points (bps) on impact. The solid lines represent posterior median estimates, while the shaded areas indicate the 68/80/90 percent credible sets, respectively. The horizontal axis measures the impulse response horizon in months. The vertical axis measures deviations from the pre-shock level, either in percentage points (interest rates and interest rate differential) or percent (treasury basis, spot rate, and excess return). The VAR does not feature the interest rate differential and excess return as an endogenous variable. Rather, we compute those objects directly from the impulse responses of the other variables as follows. The interest rate differential is the difference between the foreign and U.S. interest rate, $\Delta i_{it} = i^*_{it} - i^{\$}_t$. For the excess return, we consider the following strategy in response to a shock: An investors borrows in foreign currency for three months, exchanges it for the U.S. dollar, holds the U.S. Treasury bills for three months, and exchanges the interest rate returns on the U.S. dollar back for foreign currency three months later. The definition of the excess return is thus $rx_{it} = i^*_{it} - i^{\$}_t - \Delta s_{it+3}$.

In order to inspect relevant transmission mechanisms, we extend the baseline model. We use a measure of global economic activity[14], the Chicago Board Options Exchange Volatility Index (VIX), the global financial cycle factor of Miranda-Agrippino and Rey (2020), capital flows measured by inflows (as ratio to real GDP) provided by Avdjiev et al. (2022) and the risk aversion and uncertainty indicator by Bekaert, Engstrom and Xu (2022). We add one variable at a time to the model and report the impulse response functions of the added variables in Fig. 5. The remaining impulse response functions (of the variables in the baseline model) are shown in Fig. C1 in the appendix. These do not strongly deviate from the ones of the baseline model.

[14]We use the global industrial production index of the database of global economic indicators by the Federal Reserve Bank of Dallas.

Figure 5: Impulse Responses of the Extensions.

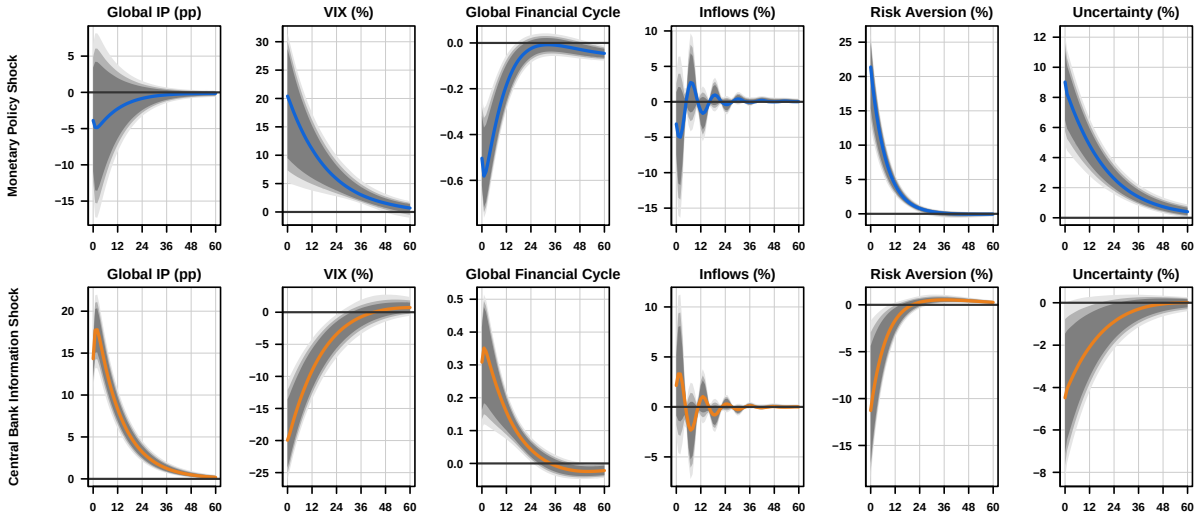

Notes: The upper panel shows the impulse responses to the U.S. monetary policy shock, while the lower panel shows the impulse responses to the central bank information shock. Estimation is based on the group-mean estimator of the linear VAR model. Solid lines represent posterior median estimates, shaded areas indicate 68/80/90 percent credible sets. Horizontal axis measures time in months. Vertical axis measures deviation from pre-shock level in percent (%) or percentage points (pp).

A contractionary monetary policy shock elicits a jump in both the U.S. and foreign interest rate, gradually returning to zero over the next 3-4 years. The U.S. interest rate even reverses and turns negative after three years. The implied interest rate differential is positive throughout the horizon. The increase in the U.S. interest rate leads to a strong appreciation of the U.S. dollar vis-à-vis the foreign currency before the U.S. dollar starts returning to the pre-shock level. On impact, the dollar appreciates almost 4 percent in value before starting to depreciate. This is in line with the overshooting hypothesis of Dornbusch (1976) although we do not find evidence of *delayed* overshooting behavior.[15] The Treasury basis strongly declines on impact before turning positive after about one year. A conventional contractionary monetary policy shock leads to a deterioration in the outlook for economic activity, investors flee to quality and switch to safer assets during times of high uncertainty. This is supported by the strong increase in risk aversion and uncertainty index while triggering a strong capital outflow towards U.S. assets after the monetary policy shock depicted in Fig. 5. This induces an increase in the convenience yield, meaning that investors demand more safe U.S. dollar assets, which causes the sharp U.S. dollar appreciation. These results align with the findings of Jiang, Lustig and Krishnamurthy (2021). The impact on the interest rate differential is positive, although statistically insignificant in the first twelve month. It results in the insignificant excess return in the first year, supporting the validity of the uncovered interest rate parity. After twelve months, the U.S. excess returns turn positive, indicating strong deviations from the uncovered interest rate parity.

[15]The pattern of delayed overshooting refers to the empirical tendency that the domestic currency appreciates over a protracted period, before it starts to depreciate (Eichenbaum and Evans, 1995; Scholl and Uhlig, 2008). As pointed out by Kim, Moon and Velasco (2017), delayed overshooting is primarily a phenomenon of the 1980s. This is in line with our evidence, given that the sample period of each currency model starts only in the post-Volcker period.

A restrictive surprise associated with a central bank information shock elicits an increase of foreign interest rates in a hump-shaped manner. Since the U.S. interest rate reacts stronger on impact, the interest rate differential is clearly negative on impact. The U.S. interest rate gradually returns back to zero within four years but does not switch signs compared to the reaction to the monetary policy shock. Foreign interest rates, however, show a more hump-shaped response, increasing further up to two years after the shock before starting to decrease again. This even causes a sign switch of the interest rate differential after two years. Following the central bank information shock, the Treasury basis does not react, while the U.S. dollar depreciates by about 1.5% before starting to appreciate back to pre-shock levels. This is in line with Pinchetti and Szczepaniak (2023), who highlight that this arises as an endogenous response to changes in investors' risk assessment of the economy. Our findings in Fig. 5 align with this explanation. The central bank information shock leads to enhanced economic activity and improved financial conditions and a reduction in risk aversion. When the Fed releases positive news about the state of the economy, an increase in the U.S. interest rate is associated with reduced market uncertainty and a reduction of investors' risk aversion. Investors search for higher returns and invest in the foreign currency, leading to a dollar depreciation and strong outflows from U.S. assets. The excess returns are largely driven by the strong negative interest rate differential in the beginning, resulting in positive returns fading out in the first year.

In a next step, we analyze the cross-sectional nature of the responses. In what follows, we report the *absolute maximum response* for each variable in the VAR (and those computed ex post). For each impulse response function, we thus take the absolute maximum value for both shocks over the full impulse response horizon. We report the results for each currency including the respective confidence bounds in Fig. 6. As imposed in the identification, both shocks elicit an increase in the U.S. interest rate. For most currencies, this also leads to an increase in the foreign interest rates, with varying strength. An outlier, although insignificant, are the Japanese yen and the Australian dollar. A contractionary monetary policy shock leads to a decrease in the Treasury basis, confirming the special role of the U.S. during times of economic uncertainty against all currencies in our sample (however, the positive reaction of ZAR is insignificant). However, the impact of the central bank information shock is indistinguishable from zero for the majority of currencies. For GBP and JPY, we observe a significant decrease in the Treasury basis to an information shock. The contractionary monetary policy shock generally results in the appreciation of the U.S. dollar, with the sole exception of GBP. In contrast, an information shock associated with a monetary tightening leads to U.S. dollar depreciation with the exception of CHF, JPY, and PHP. The impact of both shocks is very similar for the safe-haven currencies (Swiss franc and Japanese yen), leading to a U.S. dollar appreciation but with a smaller magnitude compared to other currencies. The Philippine peso also depreciates due to the information shock, possibly as a consequence of covering the Asian financial crisis in our sample. The impact on the interest rate differential is consistent across both types of shocks for most currencies, with the exception of emerging market currencies, such as CZK, MXN, PHP, and ZAR. This suggests that U.S. monetary policy tightening has a greater impact on foreign currency interest rates compared to U.S. rates. Since the excess returns are mainly driven by the currency appreciation, the monetary policy shock consistently leads to the increase in the U.S. excess returns. The reactions to an information shock are negative throughout, except for two safe-haven currencies: the Swiss franc and Japanese yen.

The linear model provides evidence that reactions to the two shocks may be currency specific, especially for high-yield and safe-haven currencies. Given the presence of interest differentials, one can expect pronounced currency carry trade activity, which is especially sensitive to unexpected changes in monetary policy. Hence, we proceed with a non-linear VAR, to analyze currency reactions to monetary policy and information shocks conditional on the respective carry trade activity.

4.3 Evidence from the Non-Linear VAR Model

Since the VAR results demonstrate the difference in adjustment dynamics for high-interest and low-interest rate currencies, we proceed with a threshold vector autoregression analysis. In the non-linear approach, we differentiate between three regimes defined by the carry trade activity measured by the currency-specific NOI_t and infer their thresholds from the data. Being a measure of actual open currency trades due to speculative motives, it conveniently carries the information how much speculative activity is present in the respective currency market. This allows us to investigate the transmission of monetary policy and central bank information shocks conditional on a currency being exposed to enhanced speculative activity. Consistent with our previous results, in what follows, we will classify the currencies in our sample into two groups. The first group is the save-haven group, consisting of CHF and JPY, whereas the second group is the high-yielding group, consisting of AUD, CAD, and NZD. While we acknowledge that EUR and GBP may also be part of the safe-haven currency group, we follow Ranaldo and Söderlind (2010) and do not include them in this particular group for our analysis.[16]

Tab. 2 presents the estimated threshold parameters allocating the regimes for each individual currency and for the two currency groups. As a first result, we distinguish between *carry trade intensity*. The regime allocation confirms that CHF and JPY (and to a lesser degree GBP) are mainly used as funding currencies relative to the U.S. dollar, given that both thresholds are negative. In the first regime the carry trade intensity for save-haven currencies is thus higher. Typical investment currencies, like AUD, and NZD show only positive thresholds, indicating that in the third regime the speculative activity is elevated. These patterns are also reflected in the respective currency groups. Only for CAD and EUR we observe a change in sign of the thresholds. Excess returns of safe-haven currencies show a stronger negative mean in the higher intensity carry regime, but with almost equal standard deviations across regimes. Also the sign of the excess return's skewness switches from positive (high carry intensity regime) towards negative indicating an asymmetry. Note that in the high intensity regime for safe-haven currencies, the carry trade is becoming more attractive. This is shown by a larger positive skewness and an increase in the kurtosis. On the contrary, for the high-yielding currency sample we observe that during periods of heightened carry intensity (i.e., the third regime), skewness turns from positive to negative and kurtosis increases, while the standard deviation remains nearly unchanged. To summarize, we observe elevated crash risk indicated by large negative tail events occurring in the high carry trade intensity regime for typical investment currencies.

We also observe that most of the time, the analyzed currencies are allocated either to the first or third regime (*Share* in Tab. 2) providing evidence of their involvement in speculative carry trade activity. We now

[16]To check for different dynamic responses, we report results for the non-classified group consisting of EUR and GBP in Fig. C3 in the appendix.

Figure 6: Heterogeneity Analysis of the Maximum Responses.

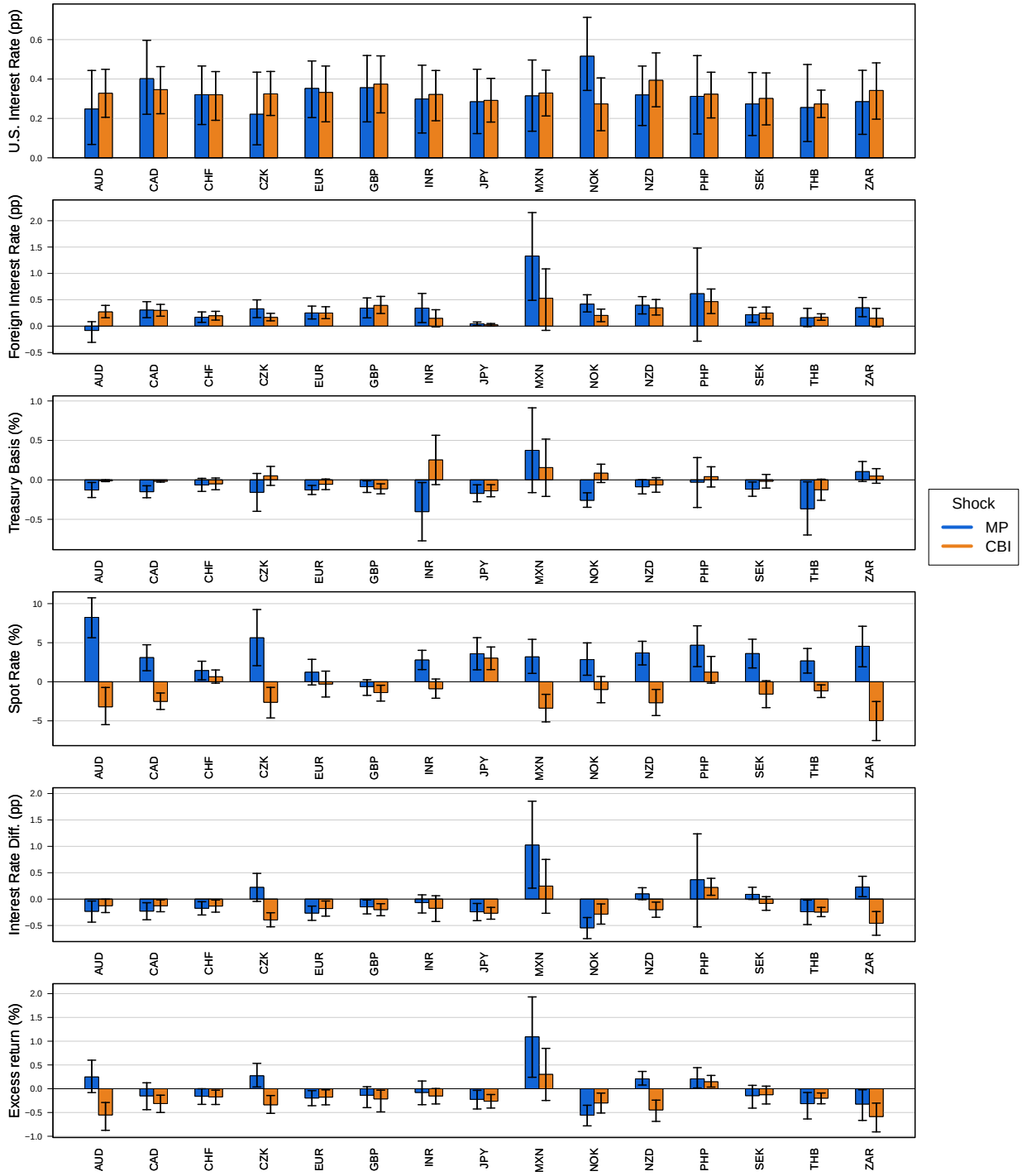

Notes: Each panel displays the maximum responses to a monetary policy (blue) and central bank information shock (orange) of one variable for each currency. Whiskers indicate 68% credible sets. Vertical axis measures the deviation from pre-shock level in percent (%) or percentage points (pp).

Table 2: Threshold Parameters and Regime-Wise Summary Statistics for Excess Returns.

	AUD	CAD	CHF	EUR	GBP	JPY	NZD	safe-haven	high-yield
γ_1	0.139	−0.006	−0.080	−0.008	−0.035	−0.154	0.168	−0.117	0.101
γ_2	0.161	0.005	−0.072	0.087	−0.010	−0.114	0.429	−0.095	0.198
Regime 1								high intensity	
Share	0.474	0.482	0.507	0.417	0.481	0.483	0.360	0.495	0.439
Mean	0.011	−0.001	0.048	−0.063	0.022	−0.121	0.027	−0.036	0.012
SD	0.203	0.143	0.174	0.161	0.17	0.186	0.249	0.180	0.199
Skewness	0.576	0.471	0.070	−0.209	−1.013	0.948	0.677	0.509	0.575
Kurtosis	4.120	3.947	3.189	2.918	6.948	5.106	4.150	4.148	4.072
Regime 3									high intensity
Share	0.485	0.505	0.481	0.433	0.490	0.459	0.36	0.470	0.450
Mean	0.078	0.002	−0.063	0.080	−0.0360	−0.081	0.061	−0.072	0.047
SD	0.236	0.137	0.196	0.158	0.165	0.202	0.180	0.199	0.185
Skewness	−1.660	−0.797	0.146	0.046	−1.230	−0.277	−0.223	−0.065	−0.894
Kurtosis	8.788	7.106	3.111	2.317	8.091	3.231	2.440	3.171	6.111

Notes: The table shows the posterior median threshold parameters, γ_1 and γ_2, and summary statistics of the currencies across the regimes (second regime omitted to enhance readability). The table reports the mean, standard deviation (SD), Skewness, and Kurtosis for monthly log excess 3-month returns, $rx_{t+3} = f_{it}^{3m} - s_{it+3}$, which is the difference between the log spot rate, s_{it+3}, and the 3-month log forward rate, f_{it}^{3m}. Mean and standard deviation are annualized and in percent. The safe-haven currency group consists of CHF and JPY, while the high-yield currency group refers to AUD, CAD, and NZD. For the details on the threshold parameter, we refer to Eq. (4.2).

Figure 7: Regime Allocation.

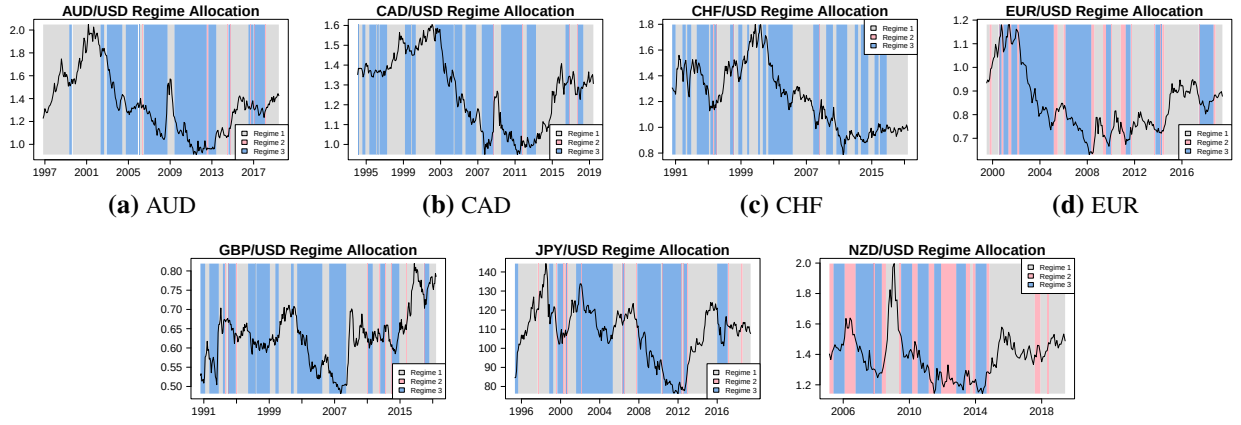

(a) AUD **(b)** CAD **(c)** CHF **(d)** EUR

(e) GBP **(f)** JPY **(g)** NZD

Notes: Each figure shows the exchange rate together with the regime allocation estimated from the threshold model Eq. (4.2). The vertical axis denotes the level of the nominal exchange rate expressed per unit of the U.S. dollar. The horizontal axis denotes the sample period. Currencies: Australian dollar (AUD), Canadian dollar (CAD), Swiss franc (CHF), Euro (EUR), Pound sterling (GBP), Japanese yen (JPY), and New Zealand dollar (NZD). Colors indicate the regime allocation where regime 1 is denoted in grey, regime 2 in light pink, and regime 3 in blue, respectively.

turn to the examination of regime allocation over time by inspecting Fig. 7. The model indicates that only the EUR and NZD enter the second regime slightly more frequently. A switch from the first to the third regime appears to coincide with episodes of U.S. dollar depreciation against the foreign currency, without spending

more than a few months in the second regime. Conversely, the transition from the third back to the first regime shows U.S. dollar appreciation, again almost immediately. For the EUR and NZD however, the transition involves staying in the second regime for several months. Thus, currencies are indeed allocated to different regimes over time and show distinct behavior in the respective regimes. We conclude that investors quickly adjust their positions to changes in the respective exchange rates. This is also confirmed when the regimes are shown as a function of the threshold, in Fig. C2. Here, we additionally see that also the safe-haven currencies, CHF and JPY, feature positive net open interest and our high-yielding currencies also negative ones. Given that we only analyze currencies against the USD, we do not take other prominent currency pairs for carry trading into account. We are now interested if the currency groups' responses to the two types of shocks depend on the regime to answer the question if carry trade activity affects monetary policy transmission.

In Fig. 8 and Fig. 9 we show the impulse response function to a contractionary monetary policy shock (upper panel) and a central bank information shock (lower panel). We report the impulse responses of the group-mean estimator of the single-currency TVAR models for the two yield groups, safe-haven and high-yielding currencies. The shock is normalized such that the U.S. interest rate increases by 25bps on impact. The black (blue) solid (dashed) lines represent the posterior median estimates, while the shaded grey (blue) areas indicate the 68/90 percent credible sets for the first (third) regime, respectively.[17] Note that carry trade intensity is elevated in the first (third) regime 1 for safe-haven (high-yield) currencies if these currencies are used as funding (investment) currency. The horizontal axis measures the impulse response horizon in months. The vertical axis measures deviations from the pre-shock level, either in percentage points (interest rates and interest rate differential) or percent (treasury basis, spot rate, and excess return). As before, the TVAR does not feature the interest rate differential and excess return as endogenous variable. We compute these objects as in the VAR analysis from the impulse responses of the other variables. As in the case of the linear model, we inspect the relevant transmission mechanisms through global economic activity, capital flows, and measures of risk aversion. We add these additional variables once at a time and re-estimate the model. Those impulse responses are reported in Fig. 10 and Fig. 11.

An increase in interest rates has different implications for the two currency groups. Safe-haven currencies are used as funding currencies while the U.S. dollar constitutes the investment currency in this trade. An increase in U.S. interest rates renders the carry trade even more attractive for these currencies. On the contrary, high-yielding currencies constitute investment currencies and the U.S. dollar is thus used as the funding currency. In this case, the potential returns of the carry trade decrease. Following a contractionary monetary policy shock, both U.S. and foreign interest rates increase and the spot rate appreciates across different regimes and currency sets. Again, the appreciation of the U.S. dollar overshoots and starts to depreciate after the initial reaction. Magnitudes of appreciations are roughly comparable to the linear specification and show small differences across currency sets and regimes. Differences arise with respect to the reaction of foreign interest rates, the implied interest rate differential, the Treasury basis, and excess returns.

[17] For the sake of readability, we do not report the 80 percent confidence bounds and abstain from reporting the impulse responses of the second regime, which can be found in Fig. C4 in the appendix. Since the model spends a considerably short time in the second regime, we deem this regime as indeterminate with respect to carry trade activity. This is supported by quite sizable confidence bands of the impulse response functions.

Figure 8: Impulse Responses of the Baseline Model: Safe-Haven Currency Group.

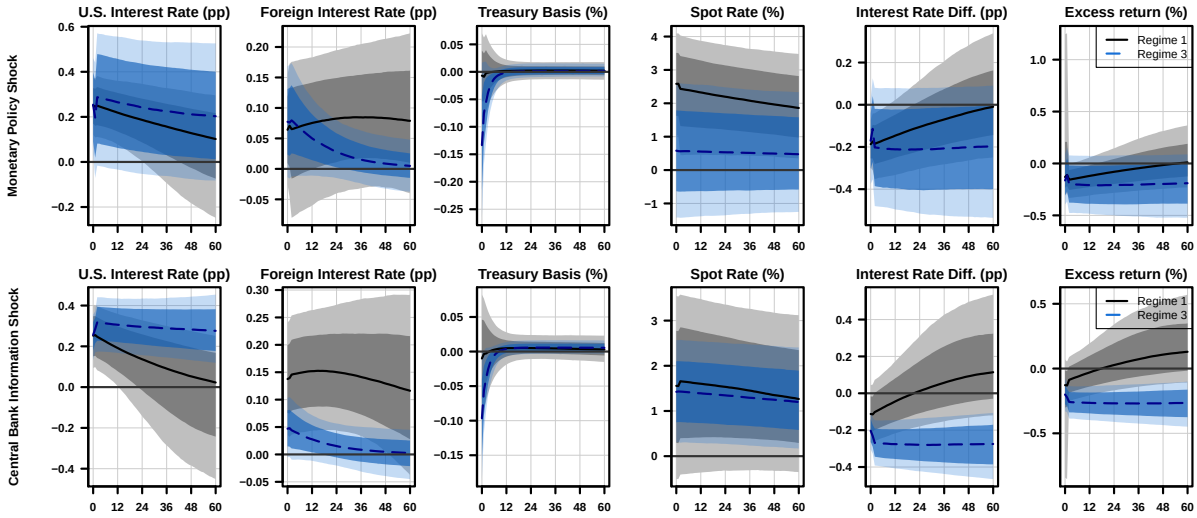

Notes: The upper panel shows the responses to an U.S. monetary policy shock, while the lower panel shows the responses to the central bank information shock. Estimation is based on the group-mean estimator of the TVAR model. Black solid (blue dashed) lines represent posterior median estimates of the first (third) regime, grey (blue) shaded areas indicate 68% and 90% credible sets of the first (third) regime. Horizontal axis measures time in months. Vertical axis measures deviation from pre-shock level in percent (%) or percentage points (pp). The safe-haven currency group consists of CHF and JPY, where the first regime corresponds to an increase in carry trade intensity when the currency is used as a funding currency.

Figure 9: Impulse Responses of the Baseline Model: High-Yield Currency Group.

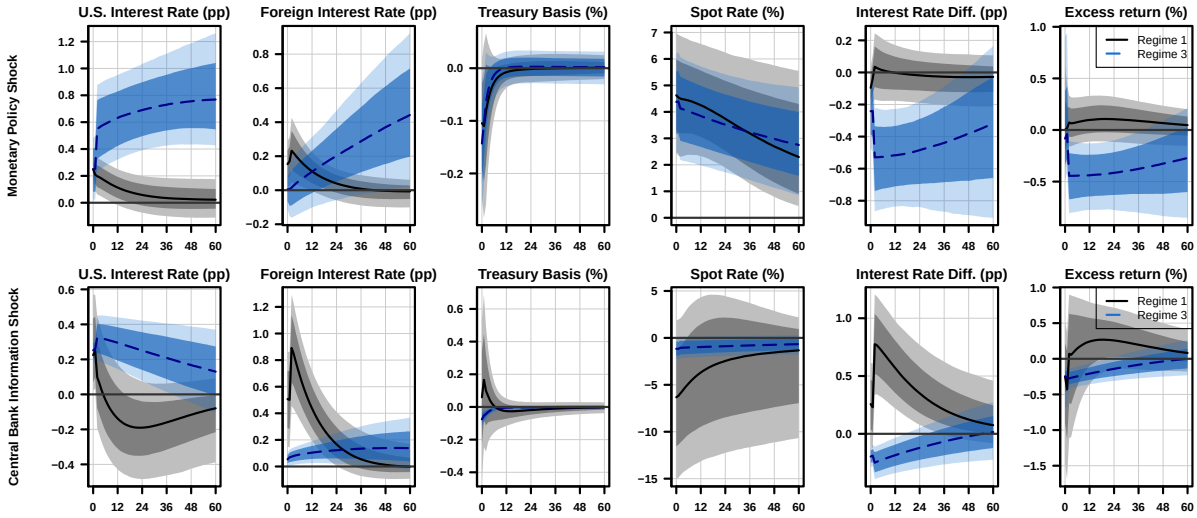

Notes: The upper panel shows the responses to the U.S. monetary policy shock, while the lower panel shows the responses to the central bank information shock. Estimation is based on the group-mean estimator of the TVAR model. Black solid (blue dashed) lines represent posterior median estimates of the first (third) regime, grey (blue) shaded areas indicate 68% and 90%we credible sets of the first (third) regime. Horizontal axis measures time in months. Vertical axis measures deviation from pre-shock level in percent (%) or percentage points (pp). The high-yield currency group consists of AUD, CAD, and NZD, where the third regime corresponds to an increase in carry trade intensity when the currency is used as an investment currency.

For safe-haven currencies, the carry trade becomes more attractive with rising U.S. interest rates due to a monetary policy shock. This holds particularly in the first regime, where the net open interest indicates that these currencies are used as funding currencies. In the first regime the carry trade intensity is elevated for this currency. Looking closer at this regime, we observe that the foreign interest rate increase more strongly compared to the third regime, in which the carry trade intensity is lower. Due to higher demand for this currency, foreign interest rates react more strongly. In line with this interpretation is the disappearance of the convenience yield of the U.S. dollar Treasuries, reflected in the negligible reaction of the Treasury basis. The spot rate reacts stronger in this regime and we observe a negative interest rate differential. We do not find evidence for positive excess returns. However, we do note that excess returns for this currency set are only marginally and with little statistical significance negative – as opposed to the linear model. When comparing this to the outcomes of the heterogeneity analysis of the linear model in Fig. 6, we observe stronger negative excess returns for these currencies. Hence, in relative terms, excess returns have indeed improved. The third regime characterizes then either low carry trade intensity or a switch to being an investment currency. Foreign interest rates show a less persistent pattern, while the Treasury basis and thus the convenience yield is significantly negative indicating higher demand for U.S. Treasuries. The appreciation of the U.S. dollar and the negative interest rate differential show high uncertainty bands. Excess returns stay consistently negative in this regime – similar to the linear model. Moreover, in terms of transmission mechanism, there are no strong differences across regimes for the extensions (as reported in Fig. 10). Risk aversion and uncertainty rises due to the monetary policy shock. If anything, risk aversion rises less strongly (or not statistically significantly) in the high carry trade intensity regime. This points to the fact that not risk aversion is driving these effects but indeed speculative trading.

The interpretation is different for the high-yield currency set. Here, the carry trade becomes less attractive due to the contractionary monetary policy shock. In this currency set, carry trade intensity is elevated in the third regime, when the currencies are used as investment currencies. Looking closer at the third regime, we observe a strong increase in both the U.S. and foreign interest rate. The strong response of the interest rates may be driven by the regime allocation of these currencies. More importantly, we observe a strong negative interest rate differential, leading to negative excess returns. While we still find an increase of the convenience yield for U.S. Treasuries in this regime, we conclude that monetary policy is strongly affecting the profitability of the carry trade. When looking at the extensions and potential mechanisms in Fig. 11, we find a similar picture as in the model with safe-haven currencies. Risk aversion and uncertainty is rising but to a lesser extent than in the low carry trade intensity model (first regime). This again points to the fact that speculative trading is driving the adjustment mechanisms rather than hedging motives, manifested in dis-investing through heightened risk aversion. In the low carry trade activity regime, we do not observe these dynamics. Interest rates react similarly in both countries causing no interest rate differential and no excess returns. While the median response of the Treasury basis is clearly negative, uncertainty bounds are large and include zero throughout the response horizon. Spot reactions do not seem to be affected by the carry trade intensity regime as they react similarly across regimes. While the spot reactions are similar, the effects in the low carry trade intensity regime are strongly accompanied by a stark risk in the VIX, a decline in the global financial cycle, and a rise in risk aversion.

Figure 10: Impulse Responses of the Extensions: Safe-Haven Currency Group.

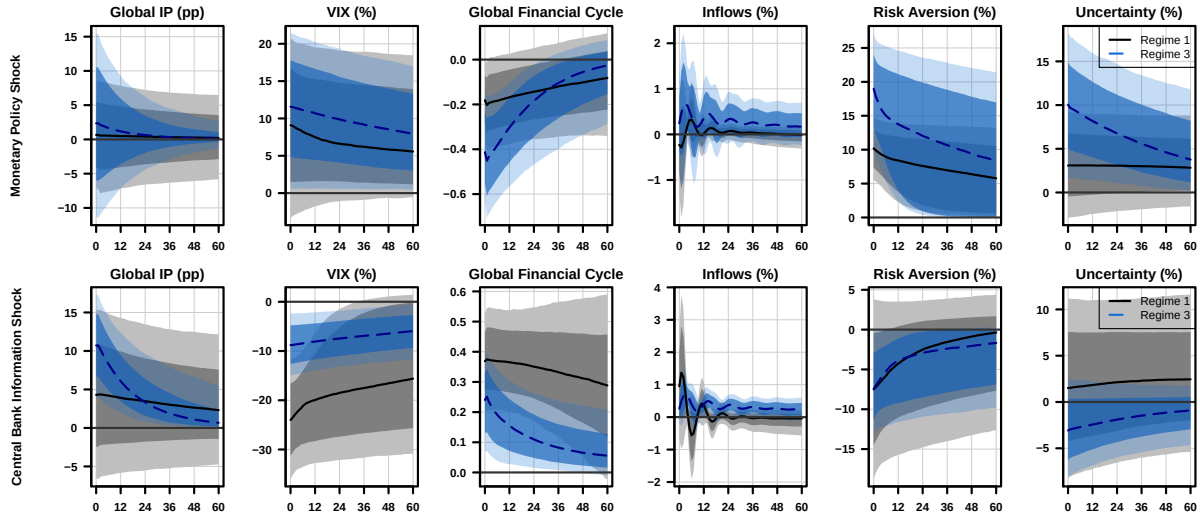

Notes: The upper panel shows the responses to an U.S. monetary policy shock, while the lower panel shows the responses to the central bank information shock. Estimation is based on the group-mean estimator of the TVAR model. Black solid (blue dashed) lines represent posterior median estimates of the first (third) regime, grey (blue) shaded areas indicate 68% and 90% credible sets of the first (third) regime. Horizontal axis measures time in months. Vertical axis measures deviation from pre-shock level in percent (%) or percentage points (pp). The safe-haven currency group consists of CHF and JPY, where the first regime corresponds to an increase in carry trade intensity when the currency is used as a funding currency.

Figure 11: Impulse Responses of the Extensions: High-Yield Currency Group.

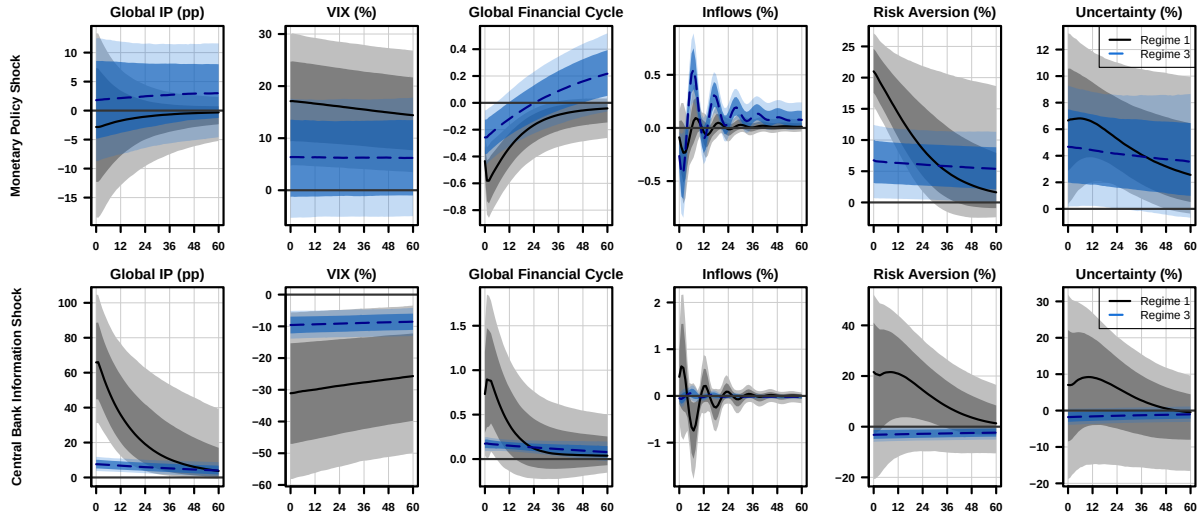

Notes: The upper panel shows the responses to the U.S. monetary policy shock, while the lower panel shows the responses to the central bank information shock. Estimation is based on the group-mean estimator of the TVAR model. Black solid (blue dashed) lines represent posterior median estimates of the first (third) regime, grey (blue) shaded areas indicate 68% and 90%we credible sets of the first (third) regime. Horizontal axis measures time in months. Vertical axis measures deviation from pre-shock level in percent (%) or percentage points (pp). The high-yield currency group consists of AUD, CAD, and NZD, where the third regime corresponds to an increase in carry trade intensity when the currency is used as an investment currency.

We turn now to the central bank information shock. For safe-haven currencies, the carry trade is again more attractive because the U.S. dollar is used as investment currency. We observe similar dynamics as in the monetary policy shock case. Since the carry trade is more attractive, an increase in the U.S. interest rate due to an information shock offers a strong response of both interest rates in the high intensity regime (first regime). The strong demand for the safe-haven currencies as funding currencies also leads to a vanishing of the convenience yield. Interestingly, the spot rate of the U.S. dollar appreciates although we observe a depreciation in the average responses of the linear model. As before in the heterogeneity analysis, the appreciation can be linked to the safe-haven status of these countries. We also find spot rate appreciations of these currencies in the linear model when comparing with Fig. 6. The interest rate differential fluctuates around zero over the impulse response horizon, leading to no negative excess returns. On the contrary, in the low carry trade intensity regime (third regime) foreign interest rates react much less pronounced. In this case, we observe a negative Treasury basis. In terms of the interest rate differential and excess returns, both display a strong negative response. In the case of the central bank information shock, these effects seem to be driven more strongly by an attenuation of risk aversion in the global financial markets, as reported in Fig. 10.

For the high-yield currency set, the carry trade becomes less attractive when the U.S. interest rates rise. In this case, the U.S. dollar is used as funding currency. The high carry trade intensity regime (third regime) shows a positive reaction of both interest rates. Foreign interest rates react less strongly and thus the differential opens up. Similar to the monetary policy shock, in the high carry trade intensity regime the Treasury basis reacts negative. This points to a consistent convenience yield of U.S. Treasuries. This regime also shows a decline in excess returns. As reported in Fig. 11, the decline in excess returns is accompanied by a smaller decline (compared to the first regime) in risk aversion and positive outlook about the economy. Again, this points to the fact that speculative trading is at play here. On the contrary, the central bank information shock in the low carry trade intensity regime (first regime) has only a short-lived effect on U.S. interest rates. Together with a positive outlook on the economy with increases on global industrial production, decreases in global uncertainty and risk as shown in Fig. 11, the interest rate differential opens up positively. However, this creates no statistically significant positive excess returns although median estimates are positive.

The results with the group of EUR and GBP, as presented in the appendix in Fig. C3, are not comparable to either group, but rather are a mixture. While the dynamic response of interest rate differentials is consistent in magnitude and shape with the group of high-yielding countries for the information shock, it does not show significant results for the monetary policy shock. This may be due to the fact that the central banks of these countries react similarly to global shocks or pursue some kind of international monetary coordination (Corsetti and Pesenti, 2005), which keeps the differentials rather small. Information shocks, on the other hand, may be asynchronous such that the interest rate differential is more pronounced. Both the responses of the treasury basis and the excess return do not match the behavior of the other two groups. The Treasury basis reacts negatively to both shocks only in the first regime, but also in the third regime for the information shock. The spot rate reacts to both shocks only in the first regime, with a depreciation of foreign currencies for a US monetary policy shock and an appreciation for an information shock. This reflects the behavior of a safe-haven currency to a monetary policy shock, while corresponding to the behavior of high-yielding currencies to an information shock.

The analysis with the non-linear model reveals that speculative carry trade activity is capable to change the transmission of monetary policy both in magnitude and shape. While it corroborates the results of the linear model, the role of currency speculation as an amplifier of monetary policy is also an important dimension. Depending on the currency set, the monetary policy shock acts differently – the U.S. dollar is used as investment (safe-haven) or funding (high-yield) currency making the carry trade more (safe-haven) or less (high-yield) attractive. Taking this into account, we observe similar dynamics in the high carry trade intensity regime. We summarize our main findings as follows. First, higher carry trade activity substantially leads to higher excess returns. The adjustment happens through the interest rate differential where we observe a strikingly different response for foreign interest rates. Second, we only find mild differences for exchange rates across regimes. Third, this holds for both currency sets and shocks. Fourth, in general risk aversion is not driving these effects. We conclude that these excess return responses are driven by speculative trading. Fifth, when looking closer at risk aversion, this channel is stronger mitigated for monetary policy shocks than for central bank information shocks.

4.4 Robustness

We provide robustness to the measurement of carry trade activity as a central element of the analysis. We redo our analysis and change the threshold indicator to the *forward premium*, a common choice when dealing with currency carry trades (see Lustig, Roussanov and Verdelhan, 2011; Menkhoff et al., 2012; Lustig, Roussanov and Verdelhan, 2014). We use the difference between the one-month forward rate, f_{it}^{1m}, and the spot rate, s_{it}, as the threshold variable. If this measure is negative constituting a *forward discount*, i.e., $(f_{it}^{1m} - s_{it}) < 0$, the currency should be sold. If there is a *forward premium*, the currency should be bought. To construct the new threshold variable, we take logs of the forward and spot and calculate the difference, which is also smoothed with an MA(5).[18] A forward premium is usually associated with the currency being used as a funding currency, while a forward discount signals that it should be chosen as an investment currency in a carry trade. The interpretation of the results remains the same, as the higher the absolute value of this measure, the more attractive a currency carry trade may become. However, the disadvantage of this measure is its lack of trading commitment. It does not separate hedging from speculative trading, nor does it imply that actual trades have been executed.

The results for the regime allocation are reported in App. D and demonstrate that the findings are generally robust to changes in the threshold variable. In particular, the two estimated thresholds are not too far apart, so the second regime does not span too far. However, some differences stand out. For our high-yielding currencies, we find a less dispersed regime distribution, so that periods of the first and third regimes are more persistent and not interrupted by regime changes. For our safe-haven currencies, we observe that the currencies are somewhat more frequently allocated to the first regime, while the Japanese yen has been in the third regime since 2009. Only for the Euro we do observe both a forward premium and a discount over the sample, which is less volatile and therefore characterized by a less dispersed regime allocation. We conclude that the results are generally robust, while some caution should be exercised when comparing the

[18] We also checked the results of subtracting the spot rate from the three month forward rate, f_{it}^{3m}, which left the results virtually unchanged.

two threshold variables. The forward premium/discount often shows periods when the overall dynamics do not show much variation. Almost all currencies show a decline in the forward premium or discount in the last years of the sample. This is not in line with the dynamics of net open interest, pointing to the importance of distinguishing between hedging and speculative trading motives, as the forward premium does not discriminate between these.

5 Trading Strategy based on Central Bank Announcements

Until now, we have shown that a monetary policy tightening surprise, accompanied by a decrease in the stock market, leads to U.S. dollar appreciation against foreign currencies. In contrast, an information shock results in U.S. dollar depreciation. Furthermore, the results of the threshold VAR indicate an additional difference based on the currency risk profile, specifically whether a currency belongs to the safe-haven or high-yield group. While it has proven to be profitable to account for monetary policy announcements when designing a currency trading strategy (see Mueller, Tahbaz-Salehi and Vedolin, 2017), we expect to be even more profitable when additionally including the *nature* of the revealed policy information in a strategy. Using this evidence, we develop an FX trading strategy in which an investor makes investment decisions on the day of the announcement, taking into consideration the joint behavior of interest rate and stock market surprises, thereby explicitly accounting for the nature of the surprise.

The investor implements thus a modified version of a currency carry trade strategy. To generate profits from this strategy, she borrows a currency with a low interest rate and invests in a currency with a high interest rate. Given the assumption of covered interest rate parity and no-arbitrage conditions, the difference between the logarithms of forward and spot rates, termed the forward discount, corresponds to the interest rate differential, $f_t - s_t \approx i_t^* - i_t$.[19] In each period t, all available currencies are sorted into three portfolios in ascending order based on their forward discounts. Each portfolio contains a third of the sample. The currencies with the highest forward discounts are assigned to Portfolio 3, while Portfolio 1 contains the third offering the lowest forward discounts. Portfolio 2 gathers the remaining currencies, which are not traded. All currencies are equally weighted within each portfolio. The carry trade strategy, known as HML (High Minus Low), exploits the interest rate differential between currency portfolios. Here the investor buys a portfolio containing currencies with high interest rate differentials and sells a portfolio containing currencies with low interest rate differentials. Given that, a carry trade investor buys currencies featuring high interest rates (Portfolio 3) and sells currencies with low interest rates (Portfolio 1) with respect to the U.S dollar, the excess return of the carry trade strategy is defined as

$$\text{HML}_{t+1} = \bar{R}_{t+1}^{P3} - \bar{R}_{t+1}^{P1}, \tag{5.1}$$

where $\bar{R}_{t+1}^{P1}$ and $\bar{R}_{t+1}^{P3}$ denote the average excess return at time $t+1$ of the Portfolio 1 and Portfolio 3, respectively.

[19] Depending on the respective strategy, we either use one-month forwards for the end-of-month strategy or weekly rolling forward contracts otherwise.

Typically, the carry trade strategy is created at the end of the month and held for the following month (see, amongst others, Lustig, Roussanov and Verdelhan, 2011; Menkhoff et al., 2012; Lustig, Roussanov and Verdelhan, 2014). Although this strategy is known for its profitability, it exhibits high volatility and negative skewness. This means that positive returns may be more frequent but lower, while losses, though less frequent, can be significantly larger. Particularly during times of economic turmoil, it tends to incur substantial losses.

The consideration of monetary policy shocks in conjunction with the carry trade strategy is of particular interest, as this strategy may be exposed to sudden losses when an unanticipated movement occurs. To mitigate this risk, we incorporate an unexpected change in the interest rate surprises and S&P 500 surprises on the day of the Fed meeting to protect the investor against severe market fluctuations. Specifically, the investor buys the U.S. dollar and sells all available currencies at time t when an increase in interest rate surprises coincides with a decline in stock market surprises on the day of the Fed meeting. Otherwise, the investor implements a conventional carry trade strategy. The portfolio is held until the next scheduled meeting. To construct the strategy, the investor uses the closing prices on the day of the announcement.

According to the uncovered interest rate parity, the investor expects the U.S. dollar to appreciate to a monetary policy shock (i.e., a positive surprise in the interest rate and a fall in stock market surprises) on the day of the Fed meeting. She uses this market signal and buys the U.S. dollar and sells all available currencies at t. The total log excess return is expressed as $-\frac{1}{N}\sum_{i=1}^{N} rx_{t+1}^{i}$ where $rx_{t+1}^{i} = f_t - s_{t+1}$ denotes the log excess return for buying the foreign currency i and selling the U.S. dollar under no-arbitrage. Otherwise, she implements the carry trade strategy (HML). As a result, the return of the new strategy, $HML^{\text{Anncmt, Shock}}$, that is created on the day of the Fed announcement and takes into consideration the shock, has the following formal expression

$$HML_{t+1}^{\text{Anncmt, Shock}} = \begin{cases} -\frac{1}{N}\sum_{i=1}^{N} rx_{t+1}^{i}, & \text{if } m_t^{\text{ff}} > 0 \ \ \& \ \ m_t^{\text{SP500}} < 0 \\ \text{HML}_{t+1}, & \text{otherwise,} \end{cases} \tag{5.2}$$

where m_t^{ff} and m_t^{SP500} correspond to surprises in the policy indicator and in the S&P 500, respectively. In what follows, we analyze the strategy performance for the whole sample, for emerging and developed markets separately, and report the cumulative returns in Fig. 12.[20]

In Tab. 3 we provide the summary statistics of the three simple carry trade portfolios (P1, P2, P3) and the extended carry trade strategy (HML) depending on the day and the signal when the portfolios are created. Panel A represents the results, when portfolios are constructed at the end of the month *without* taking the Fed's announcements into consideration. For the carry trade portfolios, returns are monotonically increasing from Portfolio 1 to Portfolio 3, resulting in an HML return of 2.7% p.a. However, the carry trade strategy exhibits high volatility, leading to a Sharpe ratio of 0.394. Furthermore, the HML returns are negatively skewed, which confirms the evidence in the literature (Brunnermeier, Nagel and Pedersen, 2008; Menkhoff et al., 2012; Dobrynskaya, 2014). If the investment strategy is created on the day of the central bank announcement and held until the next scheduled meeting instead of the end of month, a slight decrease in performance can

[20]To ensure the analysis does not begin during a period of economic turmoil, the trading exercise starts in January 2004.

Table 3: Summary Statistics of Currency Portfolios.

	P1	P2	P3	HML	HML_{DM}	HML_{EM}
Panel A: Strategy created end-of-month						
Mean	−1.109	0.867	1.592	2.701	2.382	2.474
SD	7.663	9.847	10.190	6.857	9.520	9.213
Skewness	0.020	−0.229	−0.929	−0.454	−0.841	−0.491
Kurtosis	0.061	2.020	2.453	0.158	3.144	0.768
Sharpe Ratio	−0.145	0.088	0.156	0.394	0.250	0.269
Panel B: Strategy created on the announcement day						
Mean	−2.081	−0.287	0.077	2.158	1.227	1.756
SD	6.379	6.804	9.344	6.813	8.761	6.954
Skewness	0.071	−0.113	−1.742	−0.782	−1.384	−0.440
Kurtosis	0.044	1.419	7.799	1.738	5.755	2.220
Sharpe Ratio	−0.326	−0.042	0.008	0.317	0.140	0.252
Panel C: Strategy created on the announcement day based on the shock						
Mean	−1.655	0.058	1.586	4.007	2.699	3.261
SD	4.852	4.554	6.197	4.238	5.246	6.400
Skewness	−0.014	−0.067	−0.432	0.184	0.126	0.643
Kurtosis	0.709	1.957	1.504	3.276	2.185	1.967
Sharpe Ratio	−0.341	0.013	0.256	0.945	0.514	0.510

Notes: This table shows the summary statistics of annual excess returns for the respective portfolios (P1, P2, and P3). The returns and the standard deviation are in percent. In Panel A, portfolios are constructed at the end of the month and held for one month, thus not taking Fed announcements into account. In Panel B portfolios are constructed on the day of the central bank announcement and held the day prior to the next scheduled Fed meeting. Panel C shows summary statistics of portfolios created on the day of the central bank announcement by taking into consideration the nature of the shock and held the day prior to the next scheduled Fed meeting. The sample covers the period from January 2004 until June 2019 including the whole sample of currencies. The last two columns present the summary statistics when only developed market currencies (HML_{DM}) or emerging market currencies (HML_{EM}) are included in the sample.

be seen in Panel B. However, significant improvement is observed when the strategy is created on the day of the announcement *and* is based on the nature of the shock (Panel C). As the additional signal that comes from the central bank's announcements allows to avoid periods of foreign currency depreciation, the volatility of the carry trade portfolio decreases by 2.6 percentage points annually, which leads to a Sharpe Ratio of 0.945. This is about 2.4 times higher compared to the original strategy (Panel A) and shows the superiority of our strategy. The portfolio furthermore exhibits positive skewness, drastically reducing the probability of high losses. These features are also seen in Fig. 12, which shows the cumulative returns of the respective strategies. It shows that the new strategy overcomes big losses, especially during times of high economic volatility. By taking the advantage of currency movements on the day of FOMC meetings, investors can reduce the volatility of an overall portfolio and avoid large losses, i.e., negative skewness. The results remain robust for both developed and emerging market currencies. Overall, we show that including the nature of the shock is a valuable signal for enhancing profit and helps to mitigate large losses during times of economic turmoil.

Figure 12: Cumulative Returns of Carry Trade Strategy.

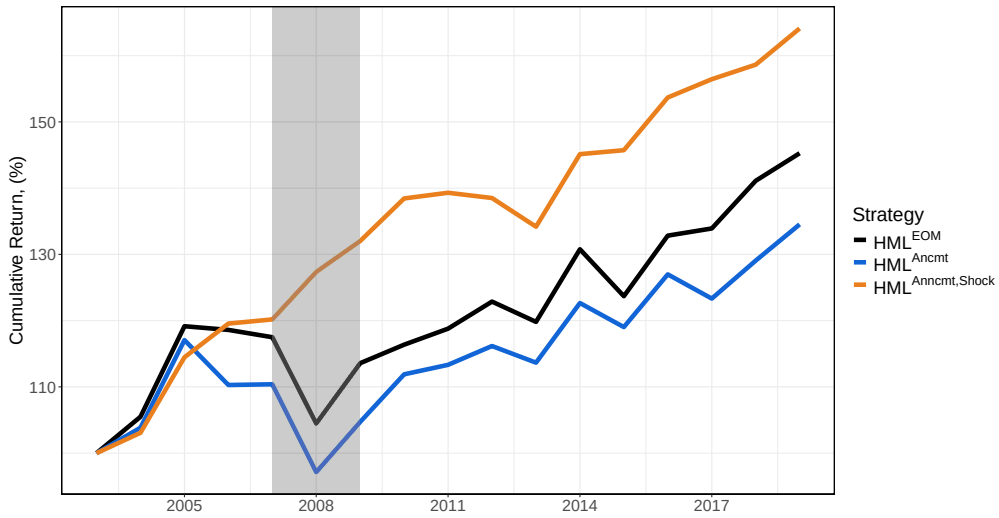

Notes: The figure shows the cumulative returns of the carry trade strategy created at the end of the month (HML^{EOM}), on the day of the central bank announcement (HML^{Ancmt}), and the carry trade strategy created on the day of the announcement that takes into consideration the co-movement between bond yields and S&P 500 prices ($HML^{Ancmt,Shock}$). Strategies are created for the period from January 2004 to June 2019 using all available currencies. The gray area corresponds to NBER recession dates.

6 Concluding Remarks

In this study, we examine the impact of U.S. monetary policy shocks on exchange rates relative to the U.S. dollar. We differentiate between conventional monetary policy and central bank information shocks. Our empirical analysis is based on a cash-flow exchange rate model, linking the U.S. dollar exchange rate to the convenience yields of U.S. Treasuries, thereby acknowledging the global importance of the U.S. dollar.

Using a linear vector autoregressive (VAR) framework, we show that the currencies react to both types of shocks with opposite signs: a monetary policy shock leads to U.S. dollar appreciation, while an information shock results in U.S. dollar depreciation. This suggests that information shocks are also transmitted through the exchange rate channel. Moving to the non-linear specification, we examine how speculative carry trade activity alters the transmission of monetary policy. The model distinguishes between three distinct regimes of carry trade activity using the net open interest on the currency futures positions of the U.S. Commodity Futures Trading Commission (CFTC). The first and third regimes correspond to high carry trade intensity given the currency's role in the carry trade, and the second regime represents an indeterminate region, accounting for the uncertainty in our threshold variable. Our findings are as follows. First, higher carry trade activity results into larger excess returns, mainly through interest rate differentials. Second, exchange rates show only mild differences across regimes. Third, these results hold across both types of shocks and currency groups. Fourth, risk aversion does not drive these effects; it suggests that speculative trading does. Fifth, risk aversion's mitigation is stronger for monetary policy shocks than for central bank information shocks. When carry trade intensity is low, strong negative responses in interest rate differentials and excess returns occur,

likely due to reduced risk aversion in global markets. Our results from the non-linear model thus strongly support the notion of currency speculation as an amplifier of monetary policy transmission.

Based on these insights, we develop a trading strategy to assess whether we can outperform the simple carry trade strategy. In a modified version, we include the information about the nature of the monetary policy shock. We find that using these signals for the portfolio creation leads to superior performance not only in terms of the Sharpe ratio and downside risks but also in higher cumulative excess returns. This strategy reduces the volatility of an overall portfolio and avoid large losses in times of financial turmoil.

To sum up, we show that the transmission of monetary policy is affected by carry trade activity. Differences arise mainly through the interest rate differential and potential excess returns, while we only find mild differences for exchange rates. This is in contrast to the sudden changes in FX markets highlighted by Brunnermeier, Nagel and Pedersen (2008). We note that their analysis is unconditional (on a specific shock) and ours is conditional on a specific set of shocks. We leave it up to further research to investigate potential other shocks, such as financial or uncertainty shocks, which may account for these features.

References

Alessandri P. and Mumtaz H. (2017) 'Financial Conditions and Density Forecasts for US Output and Inflation'. *Review of Economic Dynamics* Vol. 24, pp. 66–78.

Ang A. and Chen J. (2010) *Yield Curve Predictors of Foreign Exchange Returns*. Tech. rep. Available at SSRN: https://ssrn.com/abstract=1542342. AFA 2011 Denver Meetings Paper.

Aruoba S B. and Drechsel T. (2024) *Identifying Monetary Policy Shocks: A Natural Language Approach*. NBER Working Paper No. 32417.

Avdjiev S., Hardy B., Kalemli-Özcan Ş. and Servén L. (2022) 'Gross Capital Flows by Banks, Corporates, and Sovereigns'. *Journal of the European Economic Association* Vol. 20(5), pp. 2098–2135.

Bauer M. and Swanson E. (2023a) 'An Alternative Explanation for the "Fed Information Effect"'. *American Economic Review* Vol. 113(3), pp. 664–700.

Bauer M D. and Swanson E T. (2023b) 'A Reassessment of Monetary Policy Surprises and High-Frequency Identification'. *NBER Macroeconomics Annual* Vol. 37(1), pp. 87–155.

Bekaert G., Engstrom E C. and Xu N R. (2022) 'The Time Variation in Risk Appetite and Uncertainty'. *Management Science* Vol. 68(6), pp. 3975–4004.

Boeck M. and Mori L. (2023) *Has Globalization Changed the International Transmission of U.S. Monetary Policy?* Norges Bank Working Paper No. 15.

Boeck M. and Zörner T O. (2024) 'The Impact of Credit Market Sentiment Shocks'. *Journal of Money, Credit and Banking*, forthcoming.

Brunnermeier M K., Nagel S. and Pedersen L H. (2008) 'Carry Trades and Currency Crashes'. *NBER Macroeconomics Annual* Vol. 23(1), pp. 313–348.

Brusa F., Savor P. and Wilson M. (2020) 'One Central Bank to Rule Them All'. *Review of Finance* Vol. 24(2), pp. 263–304.

Burnside C., Eichenbaum M., Kleshchelski I. and Rebelo S. (2006) *The Returns to Currency Speculation*. NBER Working Paper No. 12489.

Burnside C., Eichenbaum M. and Rebelo S. (2007) 'The Returns to Currency Speculation in Emerging Markets'. *The American Economic Review* Vol. 97(2), pp. 333–338.

Burnside C., Eichenbaum M. and Rebelo S. (2011) 'Carry Trade and Momentum in Currency Markets'. *Annual Review of Financial Economics* Vol. 3(1), pp. 511–535.

Campbell J Y. and Clarida R H. (1987) *The Dollar and Real Interest Rates*. NBER Working Paper No. 2151.

Carvalho C M., Polson N G. and Scott J G. (2010) 'The Horseshoe Estimator for Sparse Signals'. *Biometrika* Vol. 97(2), pp. 465–480.

Chahrour R. and Valchev R. (2018) 'International Medium of Exchange: Privilege and Duty'. *Society for Economic Dynamics Meeting Papers* Vol. 317.

Chan J C. (2022) 'Asymmetric Conjugate Priors for Large Bayesian VARs'. *Quantitative Economics* Vol. 13(3), pp. 1145–1169.

Chen C W. and Lee J C. (1995) 'Bayesian Inference of Threshold Autoregressive Models'. *Journal of Time Series Analysis* Vol. 16(5), pp. 483–492.

Cieslak A., Morse A. and Vissing-Jorgensen A. (2019) 'Stock Returns Over the FOMC Cycle'. *The Journal of Finance* Vol. 74(5), pp. 2201–2248.

Cieslak A. and Schrimpf A. (2019) 'Non-Monetary News in Central Bank Communication'. *Journal of International Economics* Vol. 118, pp. 293–315.

Clarida R. and Gali J. (1994) 'Sources of Real Exchange-Rate Fluctuations: How Important Are Nominal Shocks?' *Carnegie-Rochester Conference Series on Public Policy* Vol. 41, pp. 1–56.

Corsetti G. and Pesenti P. (2005) 'International Dimensions of Optimal Monetary Policy'. *Journal of Monetary Economics* Vol. 52(2), pp. 281–305.

De Grauwe P. and Kaltwasser P R. (2012) 'Animal Spirits in the Foreign Exchange Market'. *Journal of Economic Dynamics and Control* Vol. 36(8), pp. 1176–1192.

Degasperi R., Hong S. and Ricco G. (2020) *The Global Transmission of US Monetary Policy*. CEPR Discussion Paper No. DP14533.

Della Corte P., Riddiough S J. and Sarno L. (2016) 'Currency Premia and Global Imbalances'. *The Review of Financial Studies* Vol. 29(8), pp. 2161–2193.

Dobrynskaya V. (2014) 'Downside Market Risk of Carry Trades'. *Review of Finance* Vol. 18(5), pp. 1885–1913.

Dornbusch R. (1976) 'Expectations and Exchange Rate Dynamics'. *Journal of Political Economy* Vol. 84(6), pp. 1161–1176.

Du W., Im J. and Schreger J. (2018) 'The U.S. Treasury Premium'. *Journal of International Economics* Vol. 112, pp. 167–181.

Eichenbaum M. and Evans C L. (1995) 'Some Empirical Evidence on the Effects of Shocks to Monetary Policy on Exchange Rates'. *The Quarterly Journal of Economics* Vol. 110(4), pp. 975–1009.

Falconio A. (2023) 'Carry Trades and US Monetary Policy'. *Review of International Economics* Vol. 31(1), pp. 237–248.

Faust J. and Rogers J H. (2003) 'Monetary Policy's Role in Exchange Rate Behavior'. *Journal of Monetary Economics* Vol. 50(7), pp. 1403–1424.

Faust J., Rogers J H., Wang S.-Y B. and Wright J H. (2007) 'The High-Frequency Response of Exchange Rates and Interest Rates to Macroeconomic Announcements'. *Journal of Monetary Economics* Vol. 54(4), pp. 1051–1068.

Favero C A. and Marcellino M. (2001) *Large Datasets, Small Models and Monetary Policy in Europe*. IGIER Working Papers 208. Innocenzo Gasparini Institute for Economic Research.

Follett L. and Yu C. (2019) 'Achieving Parsimony in Bayesian Vector Autoregressions with the Horseshoe Prior'. *Econometrics and Statistics* Vol. 11, pp. 130–144.

Fong W M. (2013) 'Footprints in the Market: Hedge Funds and the Carry Trade'. *Journal of International Money and Finance* Vol. 33, pp. 41–59.

Forbes C S., Kalb G R J. and Kofman P. (1999) 'Bayesian Arbitrage Threshold Analysis'. *Journal of Business & Economic Statistics* Vol. 17(3), pp. 364–372.

Frankel J A., Froot K A. et al. (1986) 'Understanding the US dollar in the Eighties: The Expectations of Chartists and Fundamentalists'. *Economic Record* Vol. 62(1), pp. 24–38.

Franz T. (2020) 'Central Bank Information Shocks and Exchange Rates'. *Deutsche Bundesbank Discussion Paper* Vol. 13/2020.

Gertler M. and Karadi P. (2015) 'Monetary Policy Surprises, Credit Costs, and Economic Activity'. *American Economic Journal: Macroeconomics* Vol. 7(1), pp. 44–76.

Goldberg L. and Tille C. (2009) 'Macroeconomic Interdependence and the International Role of the Dollar'. *Journal of Monetary Economics* Vol. 56(7), pp. 990–1003.

Gopinath G. and Stein J C. (2021) 'Banking, Trade, and the Making of a Dominant Currency'. *The Quarterly Journal of Economics* Vol. 136(2), pp. 783–830.

Gourinchas P.-O. and Rey H. (2007) 'International Financial Adjustment'. *Journal of Political Economy* Vol. 115(4), pp. 665–703.

Gürkaynak R S., Sack B. and Swanson E. (2005) 'Do Actions Speak Louder Than Words? The Response of Asset Prices to Monetary Policy Actions and Statements'. *International Journal of Central Banking* Vol. 1(1), pp. 55–93.

Haario H., Saksman E., Tamminen J. et al. (2001) 'An Adaptive Metropolis Algorithm'. *Bernoulli* Vol. 7(2), pp. 223–242.

Habib M M. and Stracca L. (2012) 'Getting Beyond Carry Trade: What Makes a Safe Haven Currency?' *Journal of International Economics* Vol. 87(1), pp. 50–64.

Hasselgren A. (2020) *Hedge Fund Herding in Currency Futures*. Tech. rep. Available at SSRN: https://ssrn.com/abstract=3544077.

Jarociński M. and Karadi P. (2020) 'Deconstructing Monetary Policy Surprises – The Role of Information Shocks'. *American Economic Journal: Macroeconomics* Vol. 12(2), pp. 1–43.

Jiang Z., Lustig H. and Krishnamurthy A. (2021) 'Foreign safe asset demand and the dollar exchange rate'. *The Journal of Finance* Vol. 76(3), pp. 1049–1089.

Kadiyala K R. and Karlsson S. (1997) 'Numerical Methods for Estimation and Inference in Bayesian VAR-Models'. *Journal of Applied Econometrics* Vol. 12(2), pp. 99–132.

Kaizoji T. (2010) *Carry Trade, Forward Premium Puzzle and Currency Crisis*. Tech. rep. Available at MPRA: https://mpra.ub.uni-muenchen.de/id/eprint/21432.

Kim S.-H., Moon S. and Velasco C. (2017) 'Delayed Overshooting: Is It an'80s Puzzle?' *Journal of Political Economy* Vol. 125(5), pp. 1570–1598.

Kim S. and Roubini N. (2000) 'Exchange Rate Anomalies in the Industrial Countries: A Solution with a Structural VAR Approach'. *Journal of Monetary Economics* Vol. 45(3), pp. 561–586.

Kuttner K N. (2001) 'Monetary Policy Surprises and Interest Rates: Evidence from the Fed funds Futures Market'. *Journal of monetary economics* Vol. 47(3), pp. 523–544.

Lunsford K G. (2018) *Understanding the Aspects of Federal Reserve Forward Guidance*. Tech. rep. Available at SSRN: https://ssrn.com/abstract=3280584.

Lustig H., Roussanov N. and Verdelhan A. (2011) 'Common Risk Factors in Currency Markets'. *The Review of Financial Studies* Vol. 24(11), pp. 3731–3777.

Lustig H., Roussanov N. and Verdelhan A. (2014) 'Countercyclical Currency Risk Premia'. *Journal of Financial Economics* Vol. 111(3), pp. 527–553.

Makalic E. and Schmidt D F. (2015) 'A Simple Sampler for the Horseshoe Estimator'. *IEEE Signal Processing Letters* Vol. 23(1), pp. 179–182.

Melosi L. (2017) 'Signalling Effects of Monetary Policy'. *The Review of Economic Studies* Vol. 84(2), pp. 853–884.

Menkhoff L., Sarno L., Schmeling M. and Schrimpf A. (2012) 'Carry Trades and Global Foreign Exchange Volatility'. *The Journal of Finance* Vol. 67(2), pp. 681–718.

Menkhoff L., Sarno L., Schmeling M. and Schrimpf A. (2017) 'Currency Value'. *The Review of Financial Studies* Vol. 30(2), pp. 416–441.

Miranda-Agrippino S. and Rey H. (2020) 'US Monetary Policy and the Global Financial Cycle'. *The Review of Economic Studies* Vol. 87(6), pp. 2754–2776.

Miranda-Agrippino S. and Ricco G. (2021) 'The Transmission of Monetary Policy Shocks'. *American Economic Journal: Macroeconomics* Vol. 13(3), pp. 74–107.

Mueller P., Tahbaz-Salehi A. and Vedolin A. (2017) 'Exchange Rates and Monetary Policy Uncertainty'. *The Journal of Finance* Vol. 72(3), pp. 1213–1252.

Nakamura E. and Steinsson J. (2018) 'High-Frequency Identification of Monetary Non-Neutrality: The Information Effect'. *The Quarterly Journal of Economics* Vol. 133(3), pp. 1283–1330.

Pesaran M H. and Smith R. (1995) 'Estimating Long-Run Relationships from Dynamic Heterogeneous Panels'. *Journal of econometrics* Vol. 68(1), pp. 79–113.

Pinchetti M. and Szczepaniak A. (2023) 'Global Spillovers of the Fed Information Effect'. *IMF Economic Review* Vol. forthcoming.

Plantin G. and Shin H S. (2006) *Carry Trades and Speculative Dynamics*. Available at SSRN: https://ssrn.com/abstract=898412.

Ranaldo A. and Söderlind P. (2010) 'Safe Haven Currencies'. *Review of Finance* Vol. 14(3), pp. 385–407.

Rogers J H., Scotti C. and Wright J H. (2018) 'Unconventional Monetary Policy and International Risk Premia'. *Journal of Money, Credit and Banking* Vol. 50(8), pp. 1827–1850.

Rubio-Ramírez J F., Waggoner D F. and Zha T. (2010) 'Structural Vector Autoregressions: Theory of Identification and Algorithms for Inference'. *The Review of Economic Studies* Vol. 77(2), pp. 665–696.

Scholl A. and Uhlig H. (2008) 'New Evidence on the Puzzles: Results from Agnostic Identification on Monetary Policy and Exchange Rates'. *Journal of International Economics* Vol. 76(1), pp. 1–13.

Sokolovski V. (2007) *Crowds, Crashes, and the Carry Trade*. preprint on webpage at https://www.dropbox.com/s/hpm4mumi9zr8m4f/CrowdsCrashesCarryTrade_SokolovskiJMP.pdf.

Spronk R., Verschoor W F. and Zwinkels R C. (2013) 'Carry Trade and Foreign Exchange Rate Puzzles'. *European Economic Review* Vol. 60, pp. 17–31.

Stavrakeva V. and Tang J. (2019) 'The Dollar During the Great Recession: US Monetary Policy Signaling and the Flight to Safety'. *CEPR Discussion Paper No.* Vol. 14034.

Zviadadze I. (2017) 'Term Structure of Consumption Risk Premia in the Cross Section of Currency Returns'. *The Journal of Finance* Vol. 72(4), pp. 1529–1566.

A Data

The results of this paper are obtained with data from various data sources. This section provides all necessary details on the data sources, transformations, and final construction in Tab. A1. Moreover, in Tab. A2 we provide an overview of the sample and our currency classification. The paper utilizes data from different sources: BIS, Datastream (WM/Reuters Barclays Bank International), Bloomberg, the Federal Reserve Bank of Dallas, the Federal Reserve Economic Data (FRED) database, and from individual websites noted further below. All series are seasonally adjusted, either by downloading the already adjusted series from the respective database or by applying a monthly X11 filter.

Table A1: Data description.

Label	Mnemonic	Description	Frequency	Transformation	Source
Policy rate	pir_t	Central bank policy rate	monthly	level	BIS
Spot rate	s_t	Spot exchange rates per unit of USD τ years ahead	monthly (eom)	level	Datastream (WM/Reuters and Barclays Bank International)
Net open interest	NOI_t	(Long-short)/Total	monthly (eom)	level	U.S. Commodity Futures Trading Commission (CFTC)
Interest rate U.S.	$i_t^{\$}$	U.S.3-month Treasury bill	monthly (eom)	level	Bloomberg
Interest rate foreign	i_t^*	Foreign 3-month Treasury rate or interbank market rate	monthly (eom)	level	Bloomberg
Yields U.S.	$y_t^{\$}$	U.S.1-year Government bond yields	monthly (eom)	level	Datastream (WM/Reuters and Barclays Bank International)
Yields foreign	y_t^*	Foreign 1-year Government bond yields	monthly (eom)	level	Datastream (WM/Reuters and Barclays Bank International)
Forward rate	f_t^1	One-year forward rate	monthly	logarithmic	Datastream (WM/Reuters and Barclays Bank International)
Treasury basis	x_t^{Treas}	according to Jiang, Lustig and Krishnamurthy (2021)	monthly	see Eq. (3.4)	constructed
GIP	gip_t	Industrial Production, World (excl. U.S)	monthly	growth rates	Database of Global Economic Indicators by the Dallas Fed
VIX	vix_t	Chicago Board Options Exchange Volatility Index	monthly	logarithmic	FRED
GFC	gfc_t	Global Financial Cycle factor by Miranda-Agrippino and Rey (2020)	monthly	level	Miranda-Agrippina's website
Inflows	$inflows_t$	capital flows as inflows to real GDP by Avdjiev et al. (2022)	monthly	level	Avdjiev et al. (2022) and Macrobond
Risk Aversion	ra_t	Risk Aversion Index by Bekaert, Engstrom and Xu (2022)	monthly	logarithmic	Nancy Xu's website
Uncertainty	unc_t	Uncertainty Index (annual volatility percentage) by Bekaert, Engstrom and Xu (2022)	monthly	logarithmic	Nancy Xu's website

Notes: (eom) denotes end-of-month.

Table A2: Sample Overview

Currency	Symbol	Start VAR	Start TVAR	DM	EM	Safe-Haven	High-Yield	Non-Classified
Australian dollar	AUD	1996-08	1996-08	✓			✓	
Canadian dollar	CAD	1993-11	1993-11	✓			✓	
Swiss franc	CHF	1990-01	1990-05	✓		✓		
Czech koruna	CZK	2000-11			✓			
Euro	EUR	1990-01	1999-04	✓				✓
Pound sterling	GBP	1990-01	1990-05	✓				✓
Indian rupee	INR	1998-09			✓			
Japanese yen	JPY	1995-02	1995-04	✓		✓		
Mexican peso	MXN	1996-11			✓			
Norwegian krone	NOK	1995-05		✓				
New Zealand dollar	NZD	1990-01	2005-01	✓			✓	
Philippine peso	PHP	1996-11			✓			
Swedish krona	SEK	1994-11		✓				
Thai baht	THB	2002-01			✓			
South African rand	ZAR	1999-01			✓			

Notes: This table gives a sample overview and the groups we used. DM stands for developed markets and EM for emerging markets. The starting dates are for the linear vector autoregressive model (VAR) and the non-linear threshold vector autoregressive model (TVAR). The currency groups, safe-haven, high-yield, and non-classified only apply for the non-linear analysis (TVAR) presented in Sec. 4.

B Estimation Details

Again, the non-linear version of the model allows for three regimes, which are distinguished by the lagged net open interest, NOI_{it-1}, the threshold variable. The threshold model with three regimes indicated by $r \in \{1, 2, 3\}$ for a specific currency i reads then as follows

$$\boldsymbol{Y}_{it} = \begin{cases} \boldsymbol{c}_{1i} + \sum_{j=1}^{p} \boldsymbol{A}_{1,ij} \boldsymbol{Y}_{it-j} + \boldsymbol{\varepsilon}_{it}, & \boldsymbol{\varepsilon}_t \sim \mathcal{N}(\boldsymbol{0}, \boldsymbol{\Sigma}_{1i}) \qquad \text{if } -\infty < NOI_{it-1} \leq \gamma_{1i}, \\ \boldsymbol{c}_{2i} + \sum_{j=1}^{p} \boldsymbol{A}_{2,ij} \boldsymbol{Y}_{it-j} + \boldsymbol{\varepsilon}_{it}, & \boldsymbol{\varepsilon}_t \sim \mathcal{N}(\boldsymbol{0}, \boldsymbol{\Sigma}_{2i}) \qquad \text{if } \gamma_1 < NOI_{it-1} \leq \gamma_{2i}, \\ \boldsymbol{c}_{3i} + \sum_{j=1}^{p} \boldsymbol{A}_{3,ij} \boldsymbol{Y}_{it-j} + \boldsymbol{\varepsilon}_{it}, & \boldsymbol{\varepsilon}_t \sim \mathcal{N}(\boldsymbol{0}, \boldsymbol{\Sigma}_{3i}) \qquad \text{if } \gamma_2 < NOI_{it-1} < \infty, \end{cases} \tag{B.1}$$

where $\boldsymbol{c}_{ri}$ $(r = 1, 2, 3)$ is an $n \times 1$ regime-specific constant, $\boldsymbol{A}_{r,ij}$ an $n \times n$ regime-specific coefficient matrix for lag j, and $\boldsymbol{\Sigma}_{ri}$ an $n \times n$ regime-specific variance-covariance matrix. Again, we estimate the model for each currency i separately. Note that it nests the linear version of the model. Both models are estimated with Bayesian techniques.

B.1 Prior Specification

In the linear VAR we have to specify priors only on the VAR coefficients, while we need to specify an additional prior distribution for the threshold parameter in the TVAR. In the TVAR, we use the same priors for the VAR coefficients as in the linear model since we estimate a linear VAR conditional on the respective regime allocation. We resort to a relatively standard independent Normal-inverse-Wishart prior setup. We abstain from using the conjugate Normal-inverse-Wishart prior, because we want to impose different priors on the own and cross-equation coefficients in the (T)VAR. Thus, we use the Horseshoe (HS) shrinkage prior on the coefficients.[21]

The prior structure of the model can be summarized as follows. Let $\boldsymbol{\alpha}_r = \text{vec}(\text{vec}\,(\boldsymbol{A}_{r1}), \ldots, \text{vec}\,(\boldsymbol{A}_{rp}))$ denote the $k \times 1$ vector of coefficients with $k = n_y(np + 1)$ for regime r. Then

$$\alpha_{rj} \mid \lambda_{rj}^2, \tau_i \sim \mathcal{N}(\underline{\alpha}_{rj}, \lambda_{rj}^2 \tau_r^2), \qquad \lambda_{rj} \sim C^+(0, 1), \qquad \tau_r \sim C^+(0, 1), \qquad j = 1, \ldots, k, \tag{B.2}$$

where $C^+(0, a)$ denotes the half-Cauchy distribution on the positive real numbers with scale parameter a. λ_{rj} denotes the *local* shrinkage parameter that is coefficient specific and τ_r is a *global* shrinkage term that pulls all elements in $\boldsymbol{\alpha}_r$ towards zero. Note that we do not impose a shrinkage prior on the deterministic coefficients. Rather, we impose a uninformative Gaussian distribution with zero mean and a large variance $(\mathcal{N}(0, 10))$ on each elements of these coefficients. Hence, $\underline{\alpha}_{rj} = 0$. The variance-covariance matrix $\boldsymbol{\Sigma}_r$ follows

$$\boldsymbol{\Sigma}_r \sim iW(\underline{\nu}, \underline{\boldsymbol{S}}), \qquad r = 1, 2, 3, \tag{B.3}$$

[21] Although Chan (2022) introduces the asymmetric conjugate prior, we abstain from using this prior due to two reasons. First, the HS shrinkage prior has proven to have excellent shrinkage properties and works well in VAR settings (Follett and Yu, 2019). Furthermore, the HS prior offers the advantage of being free of user-chosen hyperparameters. Finally, in the threshold version of the model we loose conjugacy anyway.

where $\nu = n + 2$ and $\boldsymbol{S} = \text{diag}(s_1^2, \ldots, s_n^2)$, where s_l^2 denotes the variance of the residuals of an AR(4) process of variable l ($l = 1, \ldots, n$). This is relatively standard according to Kadiyala and Karlsson (1997) and concludes the prior setup for the VAR coefficients in both models. The linear VAR follows the same prior specification, except that the regime-dependent subscript r is dropped.

In a next step, we specify the prior density on the threshold parameters $\boldsymbol{\gamma} = (\gamma_1, \gamma_2)$. While, in principle, it is sufficient to implement a rejection step in the Gibbs sampler to ensure that the inequality constraints, $\gamma_0 = -\infty$ and $\gamma_3 = +\infty$, are implicitly fulfilled, we provide a truncated prior distribution that fulfills the constraints explicitly. Thus, we use the following joint prior distribution specification for the threshold parameter, $\boldsymbol{\gamma}$:

$$\begin{aligned} \boldsymbol{\gamma} &= \prod_{j=1}^{2} p(\gamma_j \mid \gamma_{-j}), \\ \gamma_j &\sim \mathcal{TN}\left(\underline{\gamma}_j, \underline{\psi}_j^2, \gamma_{j-1}, \gamma_{j+1}\right), \end{aligned} \tag{B.4}$$

which is a truncated Normal distribution for each threshold value γ_j ($j \in \{1, 2\}$) with $\gamma_0 = -\infty$ and $\gamma_3 = +\infty$. Here, γ_{-j} denotes all elements in $\boldsymbol{\gamma}$ except γ_j. This setup roughly corresponds to Forbes, Kalb and Kofman (1999), however, with the following additional specification. The hyperparameters associated with the mean and the variance are chosen as follows. For the prior mean, we choose that $\underline{\gamma}_j = 0$ and the prior variance, $\underline{\psi}_r^2$, is a scaling factor that is set to a rather large value (in our empirical application, we specify $\psi^2 = 10^2$) but is allowed to vary over time. This allows the threshold parameters to explore the full parameter space, conditional on that the constraints $\gamma_{j-1} < \gamma_j$ are fulfilled.

B.2 Markov Chain Monte Carlo Sampler

We build a Markov Chain Monte Carlo (MCMC) algorithm to sample from the full posterior distribution. Since the conditional posterior distribution is of no well-known form, sampling this parameter is a non-trivial task. Typically, scholars achieve sampling of the relevant conditional posterior by employing a Random-Walk Metropolis-Hastings step (Chen and Lee, 1995; Alessandri and Mumtaz, 2017; Boeck and Zörner, 2024). We follow this route and are close to the sampler in Boeck and Zörner (2024). The MCMC algorithm samples iteratively from the full conditional posterior distributions. We repeat this procedure 35,000 times and discard the first 10,000 draws as burn-ins.

We obtain the joint posterior density by multiplying the likelihood with the prior. First, we define $\boldsymbol{Y}$ and $\boldsymbol{S}$ as the full history of $\boldsymbol{Y}_t$ and S_t ($t = 1, \ldots, T$). By the use of Bayes theorem we obtain

$$\begin{aligned} p(\boldsymbol{\theta}, \boldsymbol{\gamma} \mid \boldsymbol{Y}) &\propto p(\boldsymbol{Y} \mid \boldsymbol{\theta}, \boldsymbol{\gamma}) p(\boldsymbol{\theta}, \boldsymbol{\gamma}) \\ &\propto \prod_{r=1}^{R} p(\boldsymbol{Y} \mid \boldsymbol{\theta}_r) p(\boldsymbol{\theta}_r \mid \boldsymbol{S}) p(\boldsymbol{S} \mid \boldsymbol{\gamma}) p(\boldsymbol{\gamma}). \end{aligned} \tag{B.5}$$

As we rely on data augmentation, we iterate between the following two steps. First, we classify the observations into one of the regimes, and second, we draw the parameters of the model conditional on the classification.

For the classification step, we sample the group indicator $\boldsymbol{S}$ according to

$$p(\boldsymbol{S} \mid \boldsymbol{Y}, \boldsymbol{\theta}, \gamma, d) \propto p(\boldsymbol{Y} \mid \boldsymbol{S}, \boldsymbol{\theta}, \boldsymbol{\gamma}) p(\boldsymbol{S} \mid \boldsymbol{\gamma}). \tag{B.6}$$

The regime-dependent coefficients in $\boldsymbol{\theta}$ are assumed to be fixed and the indicator depends on the threshold parameter γ. The posterior density of those parameters is given by

$$p(\boldsymbol{\gamma} \mid \boldsymbol{Y}, \boldsymbol{\theta}) \propto p(\boldsymbol{Y} \mid \boldsymbol{\theta}, \boldsymbol{\gamma}) p(\boldsymbol{\gamma}). \tag{B.7}$$

Conditional on the regime indicator $\boldsymbol{S}$, sampling the regime-specific parameters $\boldsymbol{\theta}_r = (\boldsymbol{A}_r, \boldsymbol{\Sigma}_r)$ is particularly easy because we can rely on well-known conditional posterior densities of linear time series models. This results in applying Bayes theorem

$$p(\boldsymbol{\theta}_r \mid \boldsymbol{Y}, \boldsymbol{S}) \propto p(\boldsymbol{Y} \mid \boldsymbol{S}, \boldsymbol{\theta}_r) p(\boldsymbol{\theta}_r \mid \boldsymbol{S}), \quad r = 1, \ldots, 3, \tag{B.8}$$

and retrieving the posterior distribution of the regime-specific coefficients $\boldsymbol{\theta}_r$.

We employ a Gibbs sampler to draw iteratively from the joint posterior density. The resulting Markov chain is then used to inspect and analyze the posterior quantities. In the following, we will outline the individual Gibbs steps and how to draw from the conditional posterior distributions.

(i) Conditional on the regime indicator S_r, we start by sampling the regime-specific coefficients. These consist of three group of coefficients: the VAR coefficients, the associated shrinkage prior coefficients, and the variance covariance matrix. First, we gather all right-hand side variables in $\boldsymbol{X}_t = (1, \boldsymbol{m}_{t-1}', \boldsymbol{y}_{t-1}', \ldots, \boldsymbol{m}_{t-p}', \boldsymbol{y}_{t-p}')'$ and stack them into matrix form $\boldsymbol{X} = (\boldsymbol{X}_1, \ldots, \boldsymbol{X}_T)'$. Similarly, we stack $\boldsymbol{m} = (\boldsymbol{m}_1, \ldots, \boldsymbol{m}_T)'$, and $\boldsymbol{y} = (\boldsymbol{y}_1, \ldots, \boldsymbol{y}_T)'$, and $\boldsymbol{\varepsilon} = (\boldsymbol{\varepsilon}_1, \ldots, \boldsymbol{\varepsilon}_T)'$. Then, it is convenient to define $\tilde{\boldsymbol{X}}_r = \boldsymbol{D}_r \boldsymbol{X}$, $\tilde{\boldsymbol{y}}_r = \boldsymbol{D}_r \boldsymbol{y}$, $\tilde{\boldsymbol{m}}_r = \boldsymbol{D}_r \boldsymbol{m}$, and $\tilde{\boldsymbol{\varepsilon}}_r = \boldsymbol{D}_r \boldsymbol{\varepsilon}$, where $\boldsymbol{D}_r$ is a selection matrix of size $T_r \times T$ and T_r denotes the number of observations per regime r. Hence, $\tilde{\boldsymbol{X}}_r$, $\tilde{\boldsymbol{y}}_r$, and $\tilde{\boldsymbol{m}}_r$ denote all observations in the respective regime r. The VAR in matrix notation thus reads

$$\begin{pmatrix} \tilde{\boldsymbol{m}}_r & \tilde{\boldsymbol{y}}_r \end{pmatrix} = \tilde{\boldsymbol{X}}_r \begin{pmatrix} \boldsymbol{0} & \boldsymbol{A}_r \end{pmatrix} + \tilde{\boldsymbol{\varepsilon}}_r, \tag{B.9}$$

where $\boldsymbol{A}_r = \left(\boldsymbol{c}_r^y, \boldsymbol{A}_{r1}^{my}, \boldsymbol{A}_{r1}^{yy}, \ldots, \boldsymbol{A}_{rp}^{my}, \boldsymbol{A}_{rp}^{yy}\right)'$ gathers all coefficients, which have to be estimated in the VAR equation. As a last step, we denote with $\boldsymbol{\alpha}_r = \text{vec}(\boldsymbol{A}_r)$ the vectorized version of $\boldsymbol{A}_r$.

(a) We sample the VAR coefficients following Jarociński and Karadi (2020). First, we construct a diagonal $(n_y(np+1)) \times (n_y(np+1))$ prior covariance matrix $\underline{\boldsymbol{V}_i}$, where we specify the elements in step (b). This yields the following conditional posterior distribution

$$\boldsymbol{\alpha}_r \mid \Sigma_r, \tilde{\boldsymbol{y}}_r, \tilde{\boldsymbol{m}}_r \sim \mathcal{N}\left(\overline{\boldsymbol{\alpha}}_r, \overline{\boldsymbol{V}}_r\right), \tag{B.10}$$

with the posterior quantities defined as follows:

$$\overline{\boldsymbol{\alpha}_r} = \overline{\boldsymbol{V}_r}\left(\underline{\boldsymbol{V}_r^{-1}}\underline{\boldsymbol{\alpha}_r} + \left(\left(\boldsymbol{\Sigma}_r^{YY.1}\right)^{-1} \otimes \tilde{\boldsymbol{X}}_r'\right)\left(\tilde{\boldsymbol{y}}_r + \tilde{\boldsymbol{m}}_r\left(\boldsymbol{\Sigma}_r^{MM}\right)^{-1}\boldsymbol{\Sigma}_r^{MY}\right)\right) \tag{B.11}$$

and

$$\overline{\boldsymbol{V}_r} = \left(\underline{\boldsymbol{V}_r^{-1}} + \left(\boldsymbol{\Sigma}_r^{YY.1}\right)^{-1} \otimes \tilde{\boldsymbol{X}}_r'\tilde{\boldsymbol{X}}_r\right). \tag{B.12}$$

Here we use the notation $\boldsymbol{\Sigma}_r = \begin{pmatrix} \boldsymbol{\Sigma}_r^{MM} & \boldsymbol{\Sigma}_r^{MY} \\ \boldsymbol{\Sigma}_r^{YM} & \boldsymbol{\Sigma}_r^{YY} \end{pmatrix}$ and $\boldsymbol{\Sigma}_r^{YY.1} = \boldsymbol{\Sigma}_r^{YY} - \boldsymbol{\Sigma}_r^{YM}\left(\boldsymbol{\Sigma}_r^{MM}\right)^{-1}\boldsymbol{\Sigma}_r^{MY}$.

(b) Now we proceed to sample the parameters of the Horseshoe (HS) prior to construct the $k \times k$ prior variance-covariance matrix $\boldsymbol{V}_r = \text{diag}\left(\lambda_{r1}^2\tau_r^2, \ldots, \lambda_{rk}^2\tau_r^2\right)$. Makalic and Schmidt (2015) provide a simple and efficient sampling scheme based on auxiliary variables that lead to conjugate conditional posterior distributions of all parameters. Hence, we re-write the HS prior as follows. We assume that

$$\begin{aligned} \alpha_{rj} \mid \lambda_{rj}^2, \tau_i &\sim \mathcal{N}(\underline{\alpha_{rj}}, \lambda_{rj}^2\tau_r^2), \\ \lambda_{rj} &\sim C^+(0,1), \\ \tau_r &\sim C^+(0,1), \end{aligned} \tag{B.13}$$

which can be re-written by making use of the scale mixture representation of the half-Cauchy distribution. We introduce two auxiliary parameters, ν_{rj} $(j = 1, \ldots, k)$ and ξ_r and write the HS prior with the following hierarchy

$$\begin{aligned} \alpha_{rj} \mid \lambda_{rj}^2, \tau_i &\sim \mathcal{N}(\underline{\alpha_{rj}}, \lambda_{rj}^2\tau_r^2), \\ \lambda_{rj}^2 \mid \nu_{rj} &\sim \mathcal{IG}(1/2, 1/\nu_{rj}), \\ \tau_r^2 &\sim \mathcal{IG}(1/2, 1/\xi_r), \\ \nu_{r1}, \ldots, \nu_{rk}, \xi_r &\sim \mathcal{IG}(1/2, 1). \end{aligned} \tag{B.14}$$

The conditional posterior distributions for the local and global hypervariances are also inverse-Gamma distributed and look as follows

$$\lambda_{rj}^2 \mid \alpha_{rj}, \tau_r^2, \nu_{rj} \sim \mathcal{I}G\left(1, \frac{1}{\nu_{rj}} + \frac{\alpha_{rj}^2}{2\tau_r^2}\right), \qquad j = 1, \ldots, k \tag{B.15}$$

$$\tau_r^2 \mid \boldsymbol{\alpha}_r, \boldsymbol{\lambda}^2, \xi_r \sim \mathcal{I}G\left(\frac{k+1}{2}, \frac{1}{\xi_r} + \frac{1}{2}\sum_{j=1}^{k}\frac{\alpha_{rj}^2}{\lambda_{rj}^2}\right). \tag{B.16}$$

Finally, the conditional posterior distributions for the auxiliary variables are

$$\nu_{rj} \mid \lambda_j^2 \sim \mathcal{IG}\left(1, 1 + \frac{1}{\lambda_{rj}^2}\right), \qquad j = 1, \ldots, k \tag{B.17}$$

$$\xi_r \mid \tau_r^2 \sim \mathcal{IG}\left(1, 1 + \frac{1}{\tau_r^2}\right). \tag{B.18}$$

(c) Draw $\boldsymbol{\Sigma}_r$ from its conditional distribution

$$\boldsymbol{\Sigma}_r \mid \boldsymbol{A}_r, \tilde{\boldsymbol{y}}_r, \tilde{\boldsymbol{m}}_r \sim iW\left(\overline{\nu}_r, \overline{S}_r\right), \tag{B.19}$$

where $\overline{\nu}_r = \nu + T_r$ and $\overline{\boldsymbol{S}}_r = \boldsymbol{S} + \left(\begin{pmatrix}\tilde{\boldsymbol{m}}_r & \tilde{\boldsymbol{y}}_r\end{pmatrix} - \tilde{\boldsymbol{X}}_r \begin{pmatrix}\boldsymbol{0} & \boldsymbol{A}_r\end{pmatrix}\right)' \left(\begin{pmatrix}\tilde{\boldsymbol{m}}_r & \tilde{\boldsymbol{y}}_r\end{pmatrix} - \tilde{\boldsymbol{X}}_r \begin{pmatrix}\boldsymbol{0} & \boldsymbol{A}_r\end{pmatrix}\right)$.

(ii) We proceed by sampling the threshold parameter γ according to an adaptive random-walk Metropolis-Hastings step. Hereby, we follow Chen and Lee (1995) and propose a normally distributed candidate which we draw from a Gaussian, i.e., $\gamma^* \sim \mathcal{N}(\gamma^{(n-1)}, C^{(n-1)})$. $C^{(n-1)}$ is a tuning parameter and (n) denotes the n-th of N draws. The probability of accepting a candidate draw γ^* depends on the ratio of the likelihood times the prior when evaluated with the candidate and existing draw, where we reject the candidate draw if

$$\min\left[1, \frac{p(\gamma^* \mid \boldsymbol{Y}, \boldsymbol{\theta}, d) q(\gamma^*)}{p(\gamma^{(n-1)} \mid \boldsymbol{Y}, \boldsymbol{\theta}, d) q(\gamma^{(n-1)})}\right], \tag{B.20}$$

and otherwise set $\gamma^{(n)} = \gamma_c$. We follow Haario, Saksman, Tamminen et al. (2001) to adapt our tuning parameter $C^{(n)}$ by

$$C^{(n)} = \begin{cases} C_0 & \text{if } n \leq N_c, \\ s_d \text{Var}\left(\gamma^{(1)}, \ldots, \gamma^{(n-1)}\right) + s_d \eta & \text{if } n > N_c, \end{cases} \tag{B.21}$$

thereby assuming a constant tuning parameter for the first $N_c = 50$ draws and afterwards using the empirical variance to tune the MH-step. We set η to a really small number and use s_d to fine tune the algorithm to achieve acceptance probabilities between 20% and 40%. Note that this algorithm is indeed non-Markovian, but Haario, Saksman, Tamminen et al. (2001) show that this tuning algorithm has correct ergodicity properties.

C Additional Results

In this appendix, we present additional results from the linear VAR and non-linear TVAR analyses, which we chose not to include in the main text of the paper.

C.1 Additional Results of VAR Analysis

In Fig. 5 we have reported the impulse response functions of the extensions. In these extensions, we have appended an additional variable to the baseline model one-by-one in order to investigate the underlying transmission mechanisms. As a plausibility check, we also report the responses of the remaining variables of this additional estimated models in Fig. C1. We report the median response and the confidence set of the baseline model together with the median responses of each of the extended models as dashed lines. For both shocks, the responses are qualitatively similar. While the responses of the interest rates fluctuate more strongly (and given that the implied responses of the interest rate differential and the excess return), the responses of the Treasury basis and the spot rate are remarkably close to the baseline model.

Figure C1: Impulse Response Functions Comparison Baseline to Extensions.

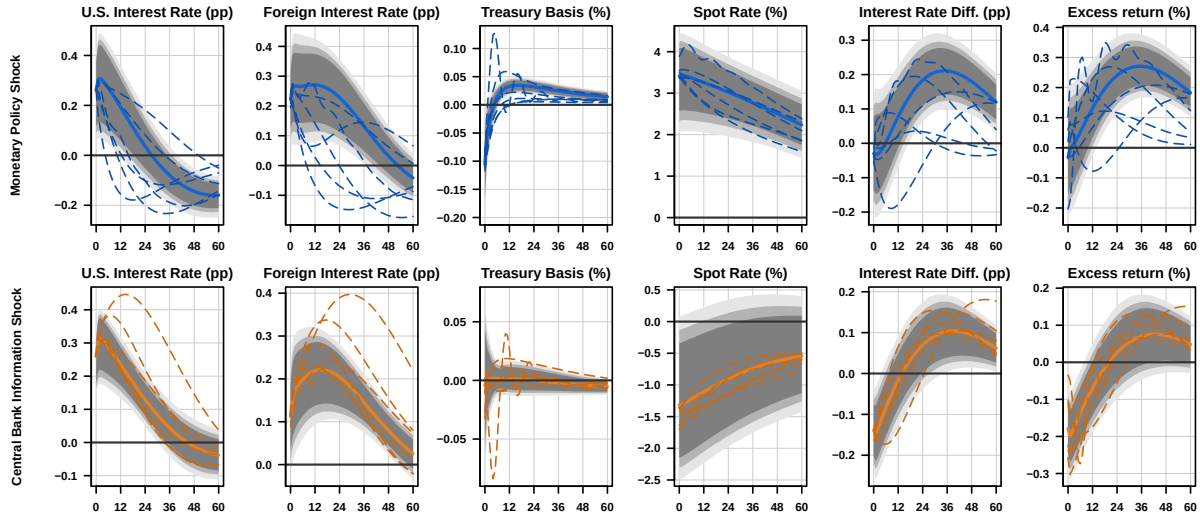

Notes: The upper panel shows the impulse responses to the U.S. monetary policy shock, while the lower panel shows the impulse responses to the central bank information shock. Estimation is based on the group-mean estimator of the linear VAR model. Solid lines represent posterior median estimates, shaded areas indicate 68/80/90 percent credible sets. Dashed lines refer to one of the models extended with one variable. Horizontal axis measures time in months. Vertical axis measures deviation from pre-shock level in percent (%) or percentage points (pp).

Figure C2: Regime Allocation as a Function of the Threshold Variable.

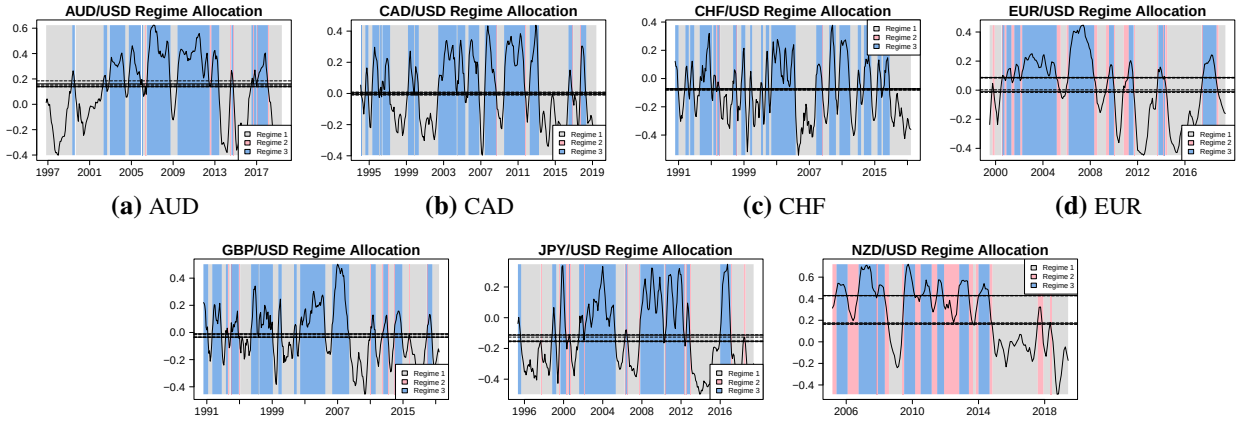

(a) AUD **(b)** CAD **(c)** CHF **(d)** EUR

(e) GBP **(f)** JPY **(g)** NZD

Notes: Each figure shows the net open interest, NOI_t (dark solid line) with the regime allocation (colors) estimated from the threshold model Eq. (4.2). The solid horizontal lines depict the thresholds together with their confidence bounds. The vertical axis denotes the net open interest. The horizontal axis denotes the sample period. Currencies: Australian dollar (AUD), Canadian dollar (CAD), Swiss franc (CHF), Euro (EUR), Pound sterling (GBP), Japanese yen (JPY), and New Zealand dollar (NZD). Colors indicate the regime allocation where the first regime is denoted in grey, the second regime in light pink, and the third regime in blue, respectively.

C.2 Additional Results of TVAR Analysis

In Fig. C2 we report the regime allocation of the estimated TVAR model in Eq. (4.2) as a function of the threshold parameter, the net open interest (left axis). The estimates of the threshold parameters, γ_1 and γ_2, are reported in Tab. 2 in the main text and shown as solid black lines in the figure along with their confidence bounds.

Fig. C3 reports the average impulse response functions of the not-classified currency group consisting of EUR and GBP, discussed in the main text.

Fig. C4 reports the average impulse response functions of the second regime for both the safe-haven and high-yield currency group. As indicated by the large size of the confidence sets, we deem the second regime as indeterminate regime. Note that we impose the same identification scheme as before. However, the time spent in this regime is rather short for each currency as indicated by the shares reported in Tab. 2 or by the light pink indicated time periods in Fig. 7 or Fig. C2.

Figure C3: Impulse Responses of the Baseline Model: Not-Classified Currency Group.

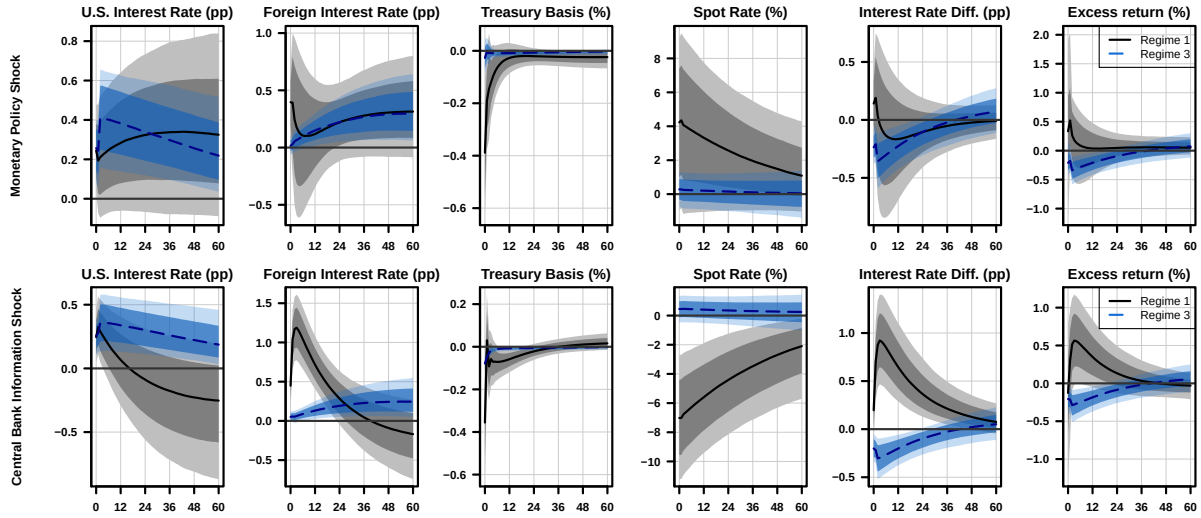

Notes: The upper panel shows the responses to the U.S. monetary policy shock, while the lower panel shows the responses to the central bank information shock. Estimation is based on the group-mean estimator of the TVAR model. Black solid (blue dashed) lines represent posterior median estimates of regime 1 (3), grey (blue) shaded areas indicate 68% and 90%we credible sets of the first (third) regime. Horizontal axis measures time in months. Vertical axis measures deviation from pre-shock level in percent (%) or percentage points (pp). The not-classified currency group consists of EUR and GBP.

Figure C4: Impulse Responses of the Baseline Model: Second Regime.

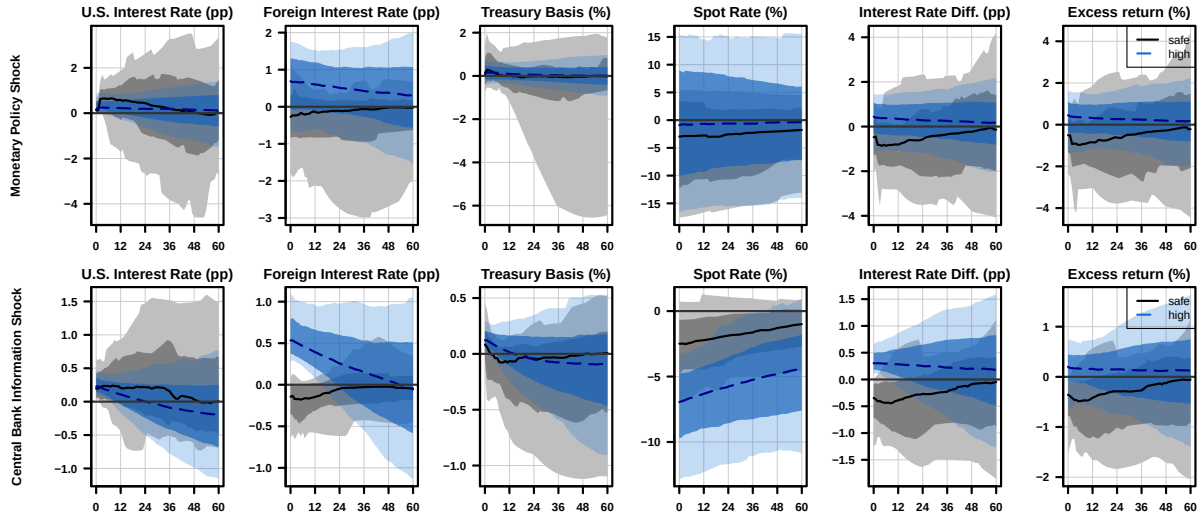

Notes: The upper panel shows the responses to an U.S. monetary policy shock, while the lower panel shows the responses to the central bank information shock. Estimation is based on the group-mean estimator of the TVAR model. Black solid (blue dashed) lines represent posterior median estimates of the second regime for the safe (high) yield currency group, grey (blue) shaded areas indicate 68% and 90% credible sets of the safe (high) yield currency group. Horizontal axis measures time in months. Vertical axis measures deviation from pre-shock level in percent (%) or percentage points (pp). The safe-haven currency group consists of CHF and JPY and the high-yield currency group consists of AUD, CAD, and NZD.

D Robustness

D.1 Robustness: Threshold Variable

We provide robustness with another threshold variable, the forward premium/discount, which we define as the difference between the 3-month log forward and log spot rates, $f_{it}^{3m} - s_{it}$. If this measure is negative, i.e., $f_{it}^{3m} - s_{it} < 0$, a *forward discount*, the currency should be sold. If there is a *forward premium*, i.e., $f_{it}^{3m} - s_{it} > 0$, the currency should be bought according to a currency carry trade trading strategy. We report summary statistics of the forward premium/discount in Tab. 1. To assess robustness, we re-estimate the non-linear version of the model for the same seven currencies: AUD, CAD, CHF, EUR, GBP, JPY, NZD. While the sample and model specification remain unchanged, we change the threshold variable to the forward premium/discount of period $t-1$, FP_{t-1}, smoothed with an MA(5).

In Fig. D1 we report the regime allocation of the estimated TVAR model in Eq. (4.2) as a function of the threshold parameter, the forward premium/discount (left axis). The total share of a currency in the second regime is slightly higher overall, while for AUD and CAD it is close to zero. For NZD, the regime allocation roughly coincides with its NOI counterpart, while regime changes from the first to the third are somewhat faster, associated with slightly less time in the second regime. For the JPY, we obtain a less dispersed regime allocation, with slightly longer transitions between the first and third regimes, as periods associated with the second regime are slightly more frequent. The JPY was in the first regime from the beginning of the sample until the beginning of 2003, and in the third regime from the end of 2008 until 2017. This is in principle consistent with the results of net open interest as a threshold, except for the period from 2013 to 2016, which was interrupted by the first regime. Here, net open interest seems to be more informative and suggests increased carry trade activity, which is not supported by the forward premium. This is especially true for the CHF, which shows a strong forward premium in the 1990s and then switches to a forward discount from 1994 onwards. While both thresholds are negative, the first regime has a slightly higher overall share compared to the baseline. Finally, the pound sterling shows a less volatile regime allocation compared to the NOI, while the overall picture is comparable. In contrast, the Euro shows a much less volatile forward premium/discount over the sample horizon and thus less dispersed regimes.

Figure D1: Regime Allocation as a Function of the Threshold Variable.

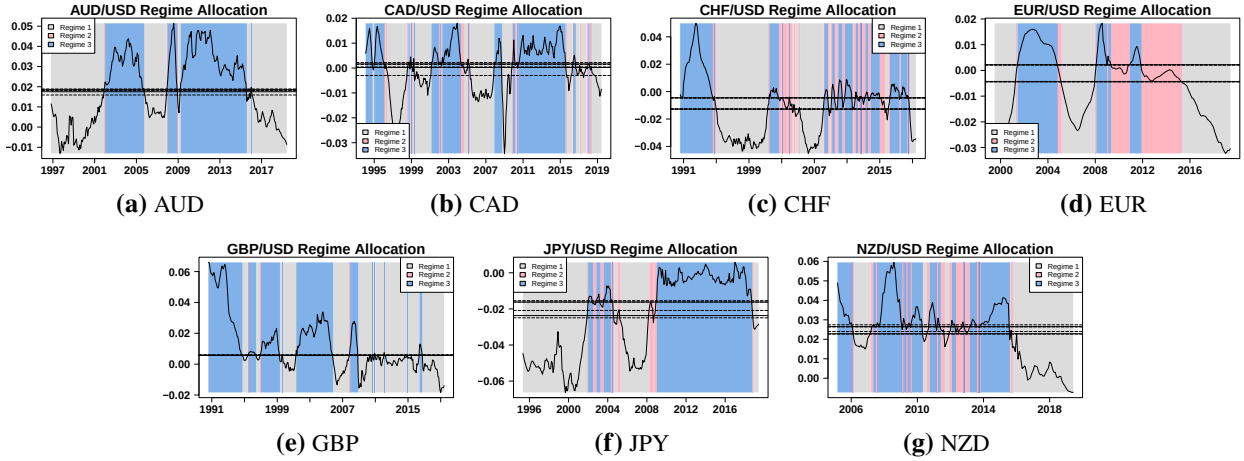

(a) AUD **(b)** CAD **(c)** CHF **(d)** EUR

(e) GBP **(f)** JPY **(g)** NZD

Notes: Each figure shows the forward premium, fp_t (dark solid line) with the regime allocation (colors) estimated from the threshold model Eq. (4.2). The solid horizontal lines depict the thresholds together with their confidence bounds. The solid line denotes the forward premium with the scale on the vertical axis. The horizontal axis denotes the sample period. Currencies: Australian dollar (AUD), Canadian dollar (CAD), Swiss franc (CHF), Euro (EUR), Pound sterling (GBP), Japanese yen (JPY), and New Zealand dollar (NZD). Colors indicate the regime allocation where the first regime is denoted in grey, the second regime in light pink, and the third regime in blue, respectively.